Unclassified **NEA/NSC/DOC(2005)15**

Organisation de Coopération et de Développement Economiques
Organisation for Economic Co-operation and Development

24-Nov-2005

English - Or. French

NUCLEAR ENERGY AGENCY
NUCLEAR SCIENCE COMMITTEE

NEA/NSC/DOC(2005)15
Unclassified

NEW INTERPRETATION OF THE NAÏADE 1 EXPERIMENTS

PART I : THE IRON AND GRAPHITE EXPERIMENTS

Jean-Claude NIMAL

JT00194842

English - Or. French

NEW INTERPRETATION OF THE NAÏADE 1 EXPERIMENTS

PART I : THE IRON AND GRAPHITE EXPERIMENTS

Jean-Claude Nimal[1]

(May-June 2005)

Abstract

Essential requirements for experimental research on neutron shielding for fission reactors are:

1. Access to an experimental facility with a pure source of fission neutrons with simple geometry, and an experimental zone. The NAÏADE 1 facility at the Commissariat à l'Energie Atomique satisfied these requirements, initially in 1957 within the Fontenay-aux-Roses reactor, and then in the reactor shielding design section (SEPP).
2. The development of a technique for measuring fast, intermediate and thermal neutron flux densities, these terms being precisely defined from a metrological standpoint.

To begin with, these experimental studies contributed to the determination of diffusion constants for two-group theory, and subsequently for qualifying computer programs and the effective cross-sections used. This very important research was sufficiently accurate for consideration now to be given for using it as a benchmark for present-day codes, such as TRIPOLI-4, which has a modelling capability, using Monte Carlo methods, that can precisely define the fission source and then qualify recent neutron cross-sections.

Thus the work we shall describe here combines the efforts of shielding designers of the 1960s with those of the present decade.

Acknowledgements

The author expresses particular thanks to the CEA/DPA/DEP/SEPP staff that has worked under the leadership of Pierre Lafore, Michel Lott in charge of the experimental management and Jean Rastoin manager of the shielding method team. The author is very grateful to Jacques Brisbois, Michel Lott, Georges Manent and Pierre Pépin who carried out the experimental work and to the CEA/DEN/DM2S/SERMA/LEPP team that developed the TRIPOLI-4 Monte-Carlo program. He thanks the OCDE/NEA staff for their helpful discussions during the present work and for the report implementation.

Note

Except where otherwise indicated, distances and dimensions are expressed in centimetres, and flux densities as particles. $cm^{-2}.s^{-1}$.

[1] Former Head of CEA Saclay SERMA/LEPP, NEA Consultant

INTRODUCTION and SUMMARY

In part A of this report we describe the NAÏADE 1 facility which contains a uranium plate irradiated by a beam of purely thermal neutrons emanating from the core of the ZOE heavy water reactor located at the Commissariat à l'Energie Atomique (CEA) at Fontenay-aux-Roses. Behind the plate, which generates fission neutrons, there is a large experimental area in which various shielding mock-ups were placed in order to validate the nuclear constants used in the computer programs and in the calculation methods themselves.

In the second part (part B) we shall deal with the concept of conventional flux density (chapter I) that is used to express the results of measurements of thermal (E<0.5eV), intermediate (between 0.5eV and a few hundred keV) and fast (above 100keV) neutron fluxes. After describing the reference block (chapter II) we shall examine the principles applied for calibrating the dosimeters used to measure the various flux densities (Chapter III). Since these calibrations involve a small number of nuclear constants that are somewhat improved in 2004 compared with 1964, we propose (Chapter IV) a reassessment of the detection coefficients of the different dosimeters (Mn55, Au197, P31, Rh103 and S32). The reassessment leads to a correction factor for each type of dosimeter which is then applied to the experimental conventional flux densities measured at the time.

In the parts C and D we describe the method of calculating the fission neutron density in the converter plate. Measurements of thermal neutron flux immediately before the fission plate are available but these are distorted by multiple diffusion in the structure and the thick natural uranium plate. The power of the plate can be checked from measurements of fast neutron flux densities behind the plate, on the mock-up side. Our approach in part C involves a subcritical source calculation using the TRIPOLI-4 program. Although the incident neutron current is entirely thermalised, the fast neutron flux density arising from the initial fissions induces secondary fissions because the plate is thick and consists of natural uranium. We give the procedure for interpreting the different experiments located in the NAÏADE 1 void. The main experiments with the void empty are interpreted with a view to verification. An attempt to estimate the neutron background noise in the void will be described.

The final two parts (E and F) are devoted to several mock-up descriptions (iron, graphite,…).
Each part contains:

- Experiment description
- Raw experimental measurements
- Corrected experimental values
- Results and comparisons based on TRIPOLI-4 calculations

PART A

DESCRIPTION OF THE NAÏADE 1 FACILITY

NAÏADE 1 is an experimental facility which has been used since 1957 for research into fission reactor shielding. It consists of the following components, starting from the core of the ZOE reactor which operates at a power of about 100 kW (see figures 1 and 2 taken from reference [1] and the primary reference [2]):

1. 8 cm of heavy water,
2. 90 cm of graphite along the axis of the facility that concerns us,
3. the outer surface of the graphite leads into a collimator structure with four successive step increases in cross-section (each section is 37.5 cm in length). The sides of the successive square sections are 50 cm, 83.3 cm, 116.7 cm and 150 cm.
4. A cadmium-brass shutter 8 cm in thickness to shield the thermal column and give access to the experimental zone at low power,
5. A boral diaphragm 1.5 cm in thickness then collimates the thermal neutron beam and offers three possible beam diameters: 60 cm, 40 cm, or 20 cm.
6. A cadmium safety shutter (2.8 mm in thickness) is used to shut off or switch on the thermal neutron beam. This cadmium shutter has an operating time of 1 second so that the length of irradiations can be determined precisely.
7. The conversion plate in which the thermal neutrons leaving the graphite produce fission neutrons. The plate is 1 square metre and the thickness of the fissile part is 2 cm. It consists of 9 square tiles 0.333 m along the side, made of natural uranium clad in 1 mm of aluminium. The total power of the plate is of the order of 2.5 W for a beam (diaphragm) diameter of 60 cm. The design reference [2] provided for 4 W for a 75 cm diaphragm, which is coherent.
8. A boral screen 15 mm in thickness is located between the converter and the void tank in which the mock-ups are positioned. This screen is intended to cut off any thermal neutrons that are back-scattered from the instrumented mock-up, with the result that the power of the fissile plate remains independent of the contents of the void. In fact, as we shall see later (parts C and D) there is a slight possibility of back-scattered epithermal, intermediate or even fast neutrons: this requires a correction factor to be applied to the power of the fissile plate that must not be neglected,
9. Then comes the void itself which is 2.5 m in depth along the axis of the converter system, with a square vertical section 3 m along each side. The void is clad by 20 mm of aluminium (the "tank"). It is surrounded laterally by an ordinary concrete wall of thickness 50 cm (at the top) to 80 cm, intended as a biological shield and to prevent neutrons escaping from the mock-up from interfering with the measurements. The vertical concrete walls also support an overhead crane that is used for positioning and moving the different parts of the mock-up. Accordingly the experimental zone has an available volume of 22 m^3 [1] with a maximum shielding thickness of 2.40 m along the axis of the converter. The overhead crane has a maximum capacity of 3 tonnes.

Various shielding mock-ups have been placed in the NAÏADE 1 facility: water, iron, different concretes, graphite, iron-water combinations, slots, shielding components from the gas-graphite type of reactor, and so on. Calibrated dosimeters [3] were used to determine the conventional flux densities at various points in the mock-ups, and were then interpreted in the counting room of the Service de Protection des Piles (SEPP) of the Commissariat à l'Energie Atomique (CEA).

Prior to the void, between the diaphragm and the NAÏADE 1 vessel, there are slots in the upper concrete to allow the penetration of rods holding dosimeters. This makes it possible to measure thermal neutron flux densities (from which the power of the fissile plate can be determined) and fast neutron flux densities (these measurements are used to verify the calculated power of the plate). These rods can be positioned to within ±2 mm [1]. The location of these rods is shown in the following table:

Rod	Position	Distance from the plane of symmetry of the plate
1	**Between plate and diaphragm**	**3.6 cm**
2	**Between Cd shutter and plate**	**2.4 cm**
3	**Before Cd shutter, reactor side**	**11.8 cm**

Table A-1

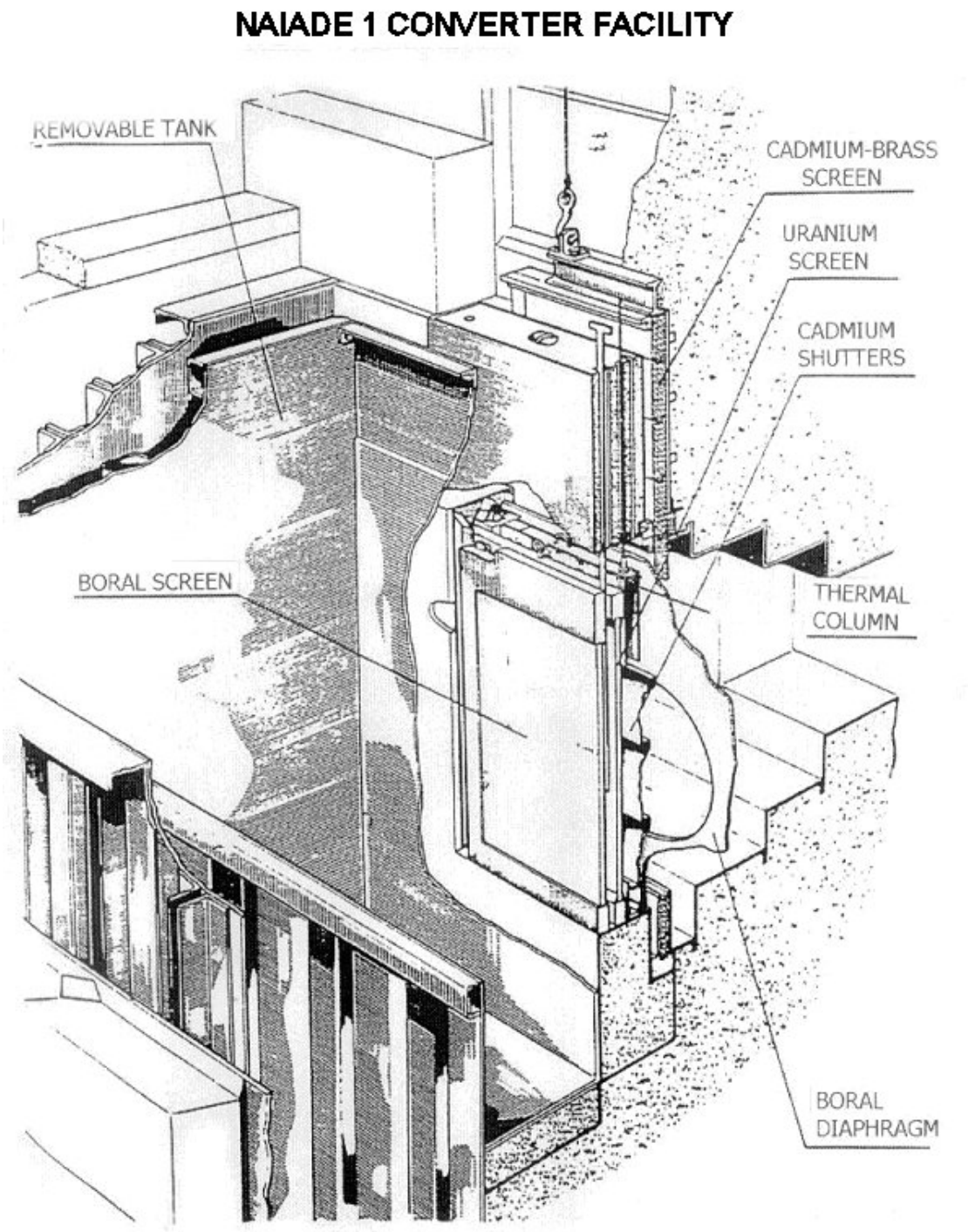
NAIADE 1 CONVERTER FACILITY
REMOVABLE TANK
CADMIUM-BRASS SCREEN
URANIUM SCREEN
CADMIUM SHUTTERS
BORAL SCREEN
THERMAL COLUMN
BORAL DIAPHRAGM

Figure 1

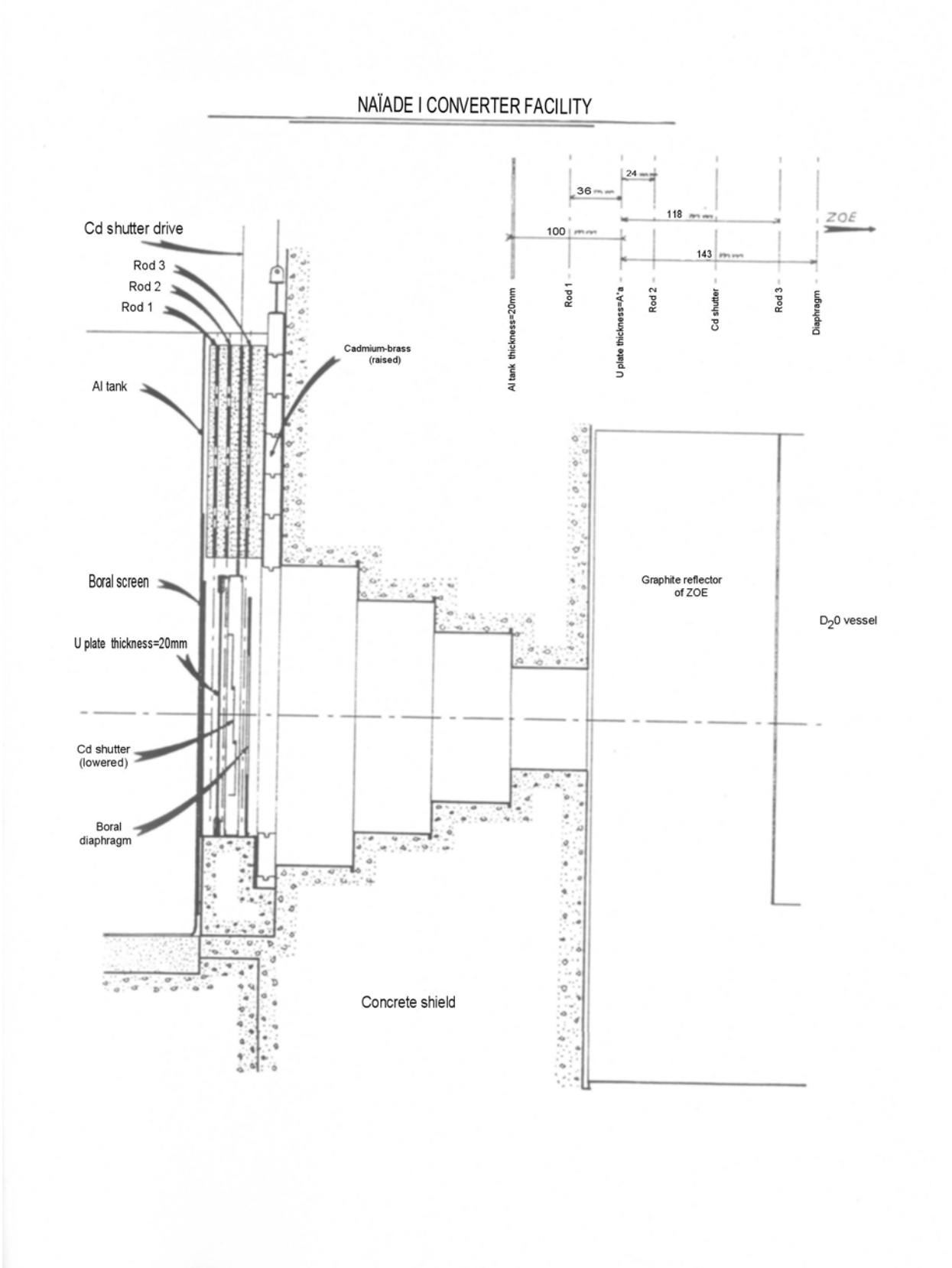
NAÏADE I CONVERTER FACILITY
24
36
118
ZOE
100
143
Al tank thickness=20mm
Rod 1
U plate thickness=A'a
Rod 2
Cd shutter
Rod 3
Diaphragm
Cd shutter drive
Rod 3
Rod 2
Rod 1
Cadmium-brass (raised)
Al tank
Boral screen
U plate thickness=20mm
Cd shutter (lowered)
Boral diaphragm
Graphite reflector of ZOE
D20 vessel
Concrete shield

Figure 2

PART B

I Introduction: expression of experimental results

This part of the report is based upon an analysis of the CEA report [3] covering measurements of flux densities of thermalised neutrons, intermediate neutrons (from 0.5eV to a few hundred keV) and fast neutrons (energies above 100keV). The authors of this substantial piece of work developed the principle of calibrating the different dosimeters in known neutron spectra. At first sight this approach looks paradoxical, because the determination of a flux density calls for a calibrated dosimeter, which in turn requires a known flux density. What the authors did was to measure a thermal neutron flux density in a reference standard block and then calibrate – with a great deal of care – first the thermal neutron dosimeters, then the intermediate neutron dosimeters and, finally, the fast neutron dosimeters, thus ensuring the coherence of the different results that are expressed in conventional flux densities, which we shall define in chapter II.

This important work was carried out in the 1960s, reaching completion in August 1964 with the publication of reference [3]. The large number of measurement campaigns, not only in the NAÏADE 1 experimental facility at Fontenay-aux-Roses but also at other sites, all involved these calibrated dosimeters.

At the time as few as possible nuclear constants were used for calibrating the dosimeters, the ones used being selected by the authors of the report because they were well known. However, their values have changed since 1960 and our intended task is to determine the correction coefficient to be applied to each measurement of conventional flux density published at the time in order to establish a coherent basis with Monte Carlo calculations done in 2003 and 2004 relative to a small number of experiments in the NAÏADE 1 facility.

First of all we shall refer to the concept of conventional flux density (chapter II): this is valuable in requiring knowledge only of the relative change of the neutron cross-section of the dosimeter as a function of energy without prejudging its absolute value which, for certain reactions, is even today open to discussion (for example: the (n,p) reaction on phosphorus 31). Today the preference is for expressing measurement results as a reaction rate $\int\sigma(E)\varphi(\vec{r},E)dE$ corresponding to the activity per atom at saturation [4]. This saturation activity - the measurement being corrected for all interference phenomena such as impurities, spurious reactions, consumption, changes in power over time, and so on – is compared directly with the reaction rate given by present-day calculations.

Chapter III briefly considers the standard source block. In chapter IV we shall investigate the principles of calibrating the different dosimeters, while chapter V is entitled “reassessing the detection coefficients and hence the conventional flux densities”. In conclusion we give a summary table of the correction coefficients.

II Expression of results: conventional flux densities

The concept of conventional flux densities for expressing the results of dosimetry measurements and of the interpreting calculations avoids, by its very nature, any consideration of the effective cross-section of the dosimeter in question. Only the variation of this effective cross-section as a function of energy is involved. We given hereunder the definition of the three conventional flux densities used for interpreting NAÏADE 1 experiments:

- The thermal flux density equivalent to 2200m/s
- The intermediate flux density by unit of lethargy defined at the energy of the main resonance
- The equivalent fission flux density.

II-1 Equivalent 2200m/s thermal flux density

This is the neutron flux density ϕ_{th} which, if the velocity of all neutrons was 2200m/s, would give the same reaction rate as the experimental flux density $\varphi(E)$. This is equation (1):

(1) $$\phi_{\mathbf{th}} = \frac{\mathbf{1}}{\sigma_{\mathbf{0}}}\int_{\mathbf{0}}^{\infty}\sigma(\mathbf{E})\varphi(\mathbf{E})\mathbf{dE}$$

σ_0 = cross-section of the dosimeter at 2200m/s

II-2 Equivalent intermediate flux density per unit of lethargy

This is the flux density per unit of lethargy ϕ_u which, if its spectrum was constant per unit of lethargy (i.e., as 1/E per unit of energy), would give the same reaction rate as the experimental spectrum $\psi(u) = E\varphi(E)$. This is equation (2):

(2) $$\phi_{\mathbf{u}} = \frac{\mathbf{1}}{\mathbf{I}} \int_{-\infty}^{\mathbf{Ucd}} \sigma(\mathbf{u})\psi(\mathbf{u})\mathbf{du}$$

where: $$\mathbf{I} = \int_{-\infty}^{\mathbf{Ucd}} \sigma(\mathbf{u})\mathbf{du}$$

II-3 Equivalent fission flux density

This is the flux density ϕ_F which, if its spectrum was proportional to the thermal fission spectrum of U235 ($s_F(E)$), would give the same reaction rate as the experimental spectrum $\varphi(E)$. This is equation (3):

(3) $$\phi_{\mathbf{F}} = \frac{\mathbf{1}}{\sigma_{\mathbf{F}}} \int_{\mathbf{0}}^{\infty} \sigma(\mathbf{E})\varphi(\mathbf{E})\mathbf{dE}$$

where $$\sigma_{\mathbf{F}} = \int_{\mathbf{0}}^{\infty} \sigma(\mathbf{E})\mathbf{s}_{\mathbf{F}}(\mathbf{E})\mathbf{dE} \quad , \quad \int_{\mathbf{0}}^{\infty} \mathbf{s}_{\mathbf{F}}(\mathbf{E})\mathbf{dE} = \mathbf{1}$$

The conventional flux densities worked out from the measurements are found from the count rates of the different dosimeters. Converting these count rates to conventional flux densities involves a coefficient B specific to the counting system (based upon the geometry, efficiency, etc.) and a characteristic coefficient d of the irradiated pellet (the "detector"). To determine these coefficients, a known flux density is needed. This is the purpose of the standard block.

III The standard source block

To begin with it is necessary to generate and determine a flux density of thermalised neutrons at ambient temperature in a large and non-absorbing environment such that the spectrum is MAXWELLIAN. This environment is called the standard block; it is described in reference [3] and a calculation has been done of how it varies very slowly with time. At the reference location of the standard block, which has a volume of $1m^3$ and consists of graphite and heavy water, there is a thermal neutron flux density equivalent to 2200m/s of 6060 n. $cm^{-2}.s^{-1}$. This reference flux density is obtained by measuring the activity of an infinitely thin Mn deposit to ensure that there is no self-absorption affecting either the thermal neutrons or the beta radiation counted. The latter were counted using a 4π counter made by juxtaposing two GEIGER-MULLER counters to within 1 mm. The cadmium ratio, indicating the purity of the thermal neutron flux density, was 65. The effective cross-section adopted for deducing this reference flux density (Mn equivalent to 2200m/s) was 13.22 b. A cross-check was done using a $\beta\gamma$ coincidence technique with gold (Au197) the effective cross-section of which was 98.8b at the time. All the flux densities given by the SEPP and resulting from the calibration are directly proportional to this value at the reference location of the standard block since the infinitely thin dosimeters were calibrated in this flux density.

IV Dosimeter calibration: principles

IV -1 Calibration of the first thermal neutron dosimeter: the reference

Once the thermal neutron flux density in the standard block is known, it is possible to calibrate a reference detector consisting of a manganese disc 20 mm in diameter with a thickness of 0.2 mm.

From the number of hits N counted during a time interval t, the conventional flux density responsible for the activation ϕ (thermal, intermediate or fast) is found using the following formula (4):

(4) $$\phi = \frac{\dfrac{\mathbf{N}}{\mathbf{1} - \mathbf{N}\pi\mathbf{t}^{-1}} - \mathbf{pt}}{(\mathbf{1} - \mathbf{e}^{-\lambda \mathbf{D}})(\mathbf{1} - \mathbf{e}^{-\lambda \mathbf{t}})\mathbf{e}^{-\lambda\theta}} \mathbf{Bd}\,\sigma$$

where

D is the duration of irradiation at constant power,

θ is the time between the end of the irradiation and the start of counting,
τ is the dead time,
p is the specific motion per unit of time,
λ is the radioactive time constant of the isotope being counted,
σ is a correction term that takes into account the drift of the counting installation and is obtained from the mean of the counts before and after measuring N for a natural uranium source (duration of each of these two counts: 5 minutes).
Bd is the product of the two factors B and d that depend respectively on the counting system and the detector being counted. Bd in particular takes the following into account:

- The self-absorption of the dosimeter for the radiation being counted
- The effective cross-section of the dosimeter,
- The self-shielding of the dosimeter (thickness, etc.),
- The geometry of the counter-dosimeter assembly.

For the reference manganese dosimeter, the thermal flux density obtaining in the standard block is known, so this dosimeter is allocated a detection coefficient d equal to 1, which makes it possible to deduce the B group coefficients for the systems of the 4π type. It will be noted that only the product Bd is involved. For the non-4π systems, a B group coefficient is determined, this depending on the geometry of the dosimeter.

IV-2 Calibration of the other thermal neutron dosimeters
The other manganese thermal neutron dosimeters are irradiated in a purely thermal flux density in the presence of the reference manganese dosimeter. It is then possible to allocate to each **a detection coefficient "d"** taking account of its specific features (mass, and so on).

NOTE: the results of the measurements using manganese dosimeters under cadmium are expressed in terms of thermal flux density equivalent to 2200m/s and not as flux density per unit of lethargy, in view of the spread of the resonances in the Mn^{55} capture reaction.

IV-3 Calibration of the reference intermediate neutron dosimeter
This consists of a deposit of gold – 0.1mg/ cm^2 – on a cellulose acetate film. The reaction Au197(n,γ)Au198 has a 1/v capture cross-section below the cadmium cut-off and a very marked resonance at 4.906eV. This detector is irradiated in the purely thermal flux density of the standard block which gives a detection coefficient d_{th} for thermal neutrons. In reference [3] the detection coefficient of this dosimeter for intermediate neutrons is calculated using the following equation (5):

(5) $$\frac{d_{\text{int}}}{d_{th}} = \frac{\sigma_0}{I}$$

Where σ_0 and I are the cross-section at 2200m/s and the resonance integral of the reaction Au197(n,γ)Au198 respectively. Irradiated under cadmium in a continuous neutron spectrum, this coefficient d_{int} and knowledge of the group B coefficient are used to define the flux density per unit of lethargy at the resonance energy of gold.

IV-4 Calibration of the other intermediate neutron dosimeters
In addition to the cadmium-sheathed gold dosimeter, an indium dosimeter is used using the (n,γ) reaction, for which there is a resonance at 1.46eV. The coefficients of the corresponding detector are obtained by irradiating the reference dosimeter and the one to be calibrated simultaneously at the same location. As far as the gold dosimeter is concerned this is straightforward, but for the indium dosimeter the flux density must be constant per unit of lethargy (1/E spectrum per unit of energy). This is done in the axial channel of ZOE. The intermediate neutron dosimeters are calibrated in this location. The spectrum requirement is satisfied in this axial channel because the scattering cross-sections of the graphite are constant as a function of energy and the effective absorption cross-section is very low [5 page 104].

IV-5 Calibration of the reference fast neutron dosimeter
The reference dosimeter involves phosphorus P31 with the P31(n,p)Si31 reaction which emits a beta particle at 1.48MeV. The question of course is how to relate the Si31 count to the equivalent fission flux density, or how to find the fast neutron detection coefficient. The answer is evident since P31 undergoes an (n,γ) reaction with thermal neutrons: P31(n,γ)P32 and the phosphorus P32 emits a beta particle of 1.7MeV. The Si31 and the P32 are therefore counted for an infinitely thin dosimeter (a deposit of 20 mg/ cm^2 of P31 on a cellulose acetate film). Self-absorption

of both betas is extremely low and also very similar owing to their very similar energies. It is therefore assumed that the counting efficiency is the same for the β of Si31 and that of P32; the error on beta absorption is of the second order and can be neglected. Reference [1] shows that the fast neutron detection coefficient of the reference phosphorus dosimeter is given by the following equation (6):

(6) $$d_{rap} = d_{th} \times \frac{\sigma_{th}}{\sigma_{rap}} \times \frac{\lambda_{rap}}{\lambda_{th}}$$

where

σ_{th} is the capture cross-section of P31 at 2200m/s,
σ_{rap} is the mean cross-section for the (n,p) reaction in the fission spectrum
λ_{rap} is the radioactive decay constant of Si31,
λ_{th} is the radioactive decay constant of P32.

Following calibration of the reference dosimeter using thermal neutrons, which gives d_{th} , equation (6) then gives the coefficient d_{rap} of the reference phosphorus dosimeter.

IV-6 Calibration of the other phosphorus dosimeters

For measuring relatively low phosphorus equivalent fission flux densities, dosimeters of a certain thickness – and not infinitely thin – are necessary. These phosphorus discs must then be calibrated. This is done in a neutron flux the spectrum of which is virtually that of fission and which is measured using the reference dosimeter. The irradiation location was located behind the converter plate of the NAÏADE 1 system at Fontenay-aux-Roses [3],[6].

IV-7 Calibration of thick fast neutron dosimeters other than the phosphorus type

Other dosimeters have been used for measuring equivalent fission flux densities for reactor shielding purposes. We may mention in particular nickel (Ni58(n,p)Co58), silicon (Si28(n,p)Al28), rhodium (Rh103(n,n')Rh103m), and sulphur (S32(n,p)P32). The disintegration paths that follow the different reactions involved in the thick dosimeters are such that the fast detector coefficients cannot be related to any known factor. Accordingly the authors of reference [3] irradiated dosimeters to be calibrated in fast neutrons along with phosphorus dosimeters having known detector coefficients, and this was done in the NAÏADE 1 converter. Due allowance was made for the fact that the NAÏADE 1 converter did not emit fast neutrons with a strictly fission spectrum. The spectrum is in fact slightly deformed because the fission neutrons are slowed down by impacts on the uranium in the converter plate. (The plate is actually made of natural uranium, 2 cm thick, with a thin aluminium cladding). A spectrum factor R_K is used to convert from the equivalent phosphorus fission flux density to the equivalent fission flux density seen by each dosimeter, from which all the detection coefficients can be deduced. This spectrum factor is defined by the following equation (7):

(7) $$R_K = \frac{\frac{1}{\sigma_{f,K}} \times \int_0^\infty \sigma_K(E)\phi(E)dE}{\frac{1}{\sigma_{f,P}} \times \int_0^\infty \sigma_P(E)\phi(E)dE}$$

where $\sigma_{f,J}$ is the mean value of the effective cross-section of the dosimeter J in the pure thermal fission spectrum of U^{235} (J = phosphorus, sulphur, nickel, etc.). $\phi(E)$ is the neutron spectrum prevailing at the measurement location. This was calculated using a Monte Carlo method. The closer the spectrum $\phi(E)$ is to the fission spectrum, the closer the spectrum factors are close to unity.

It is recalled that the calibration of the counting system+dosimeter assembly is based upon the experimental determination of Bd. All the dosimeters are calibrated on a rotating assembly that ensures that the measurements are coherent with one another

V Reassessment of the detection coefficients and hence the conventional flux densities

The methods used for calibrating dosimeters involve nuclear constants such as the effective cross-sections and half-lives of the isotopes present in the structure of the dosimeters. The detection coefficients were evaluated using the constants extant at the time the measurements on the NAÏADE 1 system were published. Since then the accepted values of these constants have changed, hence the need to reassess the conventional flux densities published from the

measurements. The points at which the nuclear constants are involved in determining the detection coefficients are recalled hereunder:

POINT A the flux density of the standard block deduced from the absolute activity of a thin deposit of manganese.

POINT B the change from the manganese dosimeter to gold (equation (5))

POINT C the change from P32 to Si31; equation (6) gives the coefficient for the reference phosphorus dosimeter

POINT D the method of spectrum factors (equation (7)) which is used to convert the phosphorus reference detection coefficient to those of other fast neutron dosimeters.

POINT A: the reference equivalent thermal flux density

Reference [3] uses an Mn55 capture cross-section at 2200m/s of 13.22b for converting from the reaction rate measured in the conventional thermal flux density to the reference location of the standard block. The value recommended by ZIJP [7] is 13.25b which corresponds to an overestimate of 0.23% in the equivalent thermal flux density [3]. In reality the problem of the absolute value of the reference flux density is not a problem for any of the experiments carried out in NAÏADE 1: there is a very small error (0.23% !) not only on all the measurements of conventional flux density but also on the fission sources in the uranium plate (see reference [1]). Indeed it would appear that an error of 0.23% can be neglected having regard to the uncertainties about the value of 13.25b given by ZIJP [7 page 76]. It is possible that those responsible for the first measurements of reference thermal flux density in the standard block have assumed the saturation case such that the period of Mn56 does not affect the activity immediately after irradiation. The period only comes into play over the time between the irradiation and the counting which is of the order of 20 minutes. The period of Mn56 used in [3] is 2.58h and the activity measurement was continued for 60 hours. This value of the period is confirmed by ZIJP: 2.577 hours.

The precision of the mass of the manganese deposit is unknown, as is that of the counting system (GEIGER-MULLER). Independent checks of the equivalent reference thermal flux density were done using the gold deposit; intercalibrations were carried out in conjunction with foreign dosimetry laboratories.

Of course any lack of precision on the reference thermal flux density in the standard block has no impact on the coherence between the measured or calculated conventional flux densities and the fission sources that create them. We shall not correct this reference value.

POINT B changing to the detector coefficient of the reference gold dosimeter

Equation (5) as given hereunder:

(5) $$\frac{d_{\text{int}}}{d_{th}} = \frac{\sigma_0}{I} = r_1$$

was applied by the authors of reference [3] using an effective cross-section of 98.8b and a resonance integral of 1583b giving r_1 = 6.241E-2

$$\frac{\mathbf{d_{int}}}{\mathbf{d_{th}}} = \frac{\sigma_0}{\mathbf{I}} = \frac{\mathbf{98.8}}{\mathbf{1583}} = \mathbf{6.241E-2}$$

where I is the resonance integral of gold and σ_0 the effective cross-section at 2200m/s. From the detection coefficient d_{int} we shall deduce the flux density per unit of lethargy at the resonance energy of gold.

In reference [7], ZIJP proposes 99.2b and 1562b for σ_0 and I respectively; ENDF/B-VI [8], a more recent evaluation that we shall use for interpreting the measurements done in NAÏADE 1 recommends the following values: 99.25b and 1565b. We shall use these values so that the ratio σ_0/I will take the value 6.342E-2. Since the conversion of the counting data to conventional flux densities is proportional to the coefficients d, we shall multiply the published experimental values by the ratio 6.342E-2/6.241E-2 = 1.016 and we shall use the ENDF/B/6 cross-sections to convert from reaction rates to conventional flux densities. In passing we may note the correction value that is very close to unity.

POINT C changing to the reference detector coefficient for fast neutrons: P31

To begin with we would point out the low influence of the uncertainty in the values for the period of P32 (14.3 days [3] compared with 14.29 days currently used) and Si31 (2.62 hours [3] compared with 2.622 hours used at present.

The first idea that presents itself for defining the factor R_2 that is used for correcting the detection coefficient of the reference phosphorus 31 fast neutron dosimeter is to employ equation (6), repeated hereunder, by examining the available values for the cross-section of P31 for the (n,γ) and (n,p) reactions.

(6) $$d_{rap} = d_{th} \times \frac{\sigma_{th}}{\sigma_{rap}} \times \frac{\lambda_{rap}}{\lambda_{th}}$$

The following table shows the considerable scatter in the values of the component R_2 of the correction.

Reference	$\frac{d_{rap}}{d_{ther}}$	σ(n,γ) mb	σ(n,p) mb	R_2
SEPP [1]	**829.6**	**190**	**30**	
ZIJP	**789.4**	**172**	**28.5**	**0.9515**
ENDF/B/6 R4	**783.2**	**199.5**	**33.32***	**0.9440**
JEF 2	**596.6**	**166.4**	**36.48**	**0.7192**
JENDL 3.2	**596.3**	**166.3**	**36.48**	**0.7188**
JENDL 3.3	**721.75**	**166.2**	**30.12**	**0.8700**
BROND 2	**711.31**	**181.2**	**33.32**	**0.8574**
CENDL 2	**732.06**	**178.2**	**31.84**	**0.8824**

Table B-1

***this value is given in reference [8]**

The second approach is to calculate the ratio R_2 from the equivalent phosphorus fission flux densities calculated behind the fission plate of the NAÏADE 1 system with great precision and using recent effective cross-sections for neutron transport (the calculation pertaining to the NAÏADE 1 system will be described in part C below). The expression for the coefficient R_2 is given by equation (6bis) hereunder:

(6bis) $$R_2 = \frac{newfastflux}{oldfastflux}$$

The coefficient R_2 is calculated using the TRIPOLI-4 Monte Carlo code [9] using effective cross-sections for the different materials taken from ENDF/B/6 R4 and with two sources for the response function for calculating the equivalent (n,p) fission flux density on phosphorus 31: ENDF/B-VI R4 and IRDF_90. The results of these calculations are given in the following table by TRIPOLI-4_XX_YY where XX is the source of the effective cross-sections for neutrons transporting the materials and YY the source of the response function of the P31(n,p) reaction. This table B-2 brings together the different values of the correction factor R_2. It is recalled that the equivalent P31 fission flux densities at rod 1 (on the axis) and next to the inner wall of the aluminium tank (on the axis) given in a number of experiments are 5.00E7 and 2.20E7 n× cm^{-2}×s^{-1} respectively. There will be no surprise at this precise figure of 5.00E7: all the measurements were normalised to this value of "plate power." The value of 2.20E7 appears reliable since a number of measurements give 2.20E7 or 2.21E7.

Reference	Equivalent fission flux density	σ(n,p) mb	R_2
TRIPOLI-4_B6_B6 Next to fissile plate	**4.0640E7±0.22%**	**33.73****	**0.813**
TRIPOLI-4_B6_B6 Next to inside of tank	**1.8226E7±0.25%**	**33.73****	**0.8280**
TRIPOLI-4_B6_IRDF90 Next to fissile plate	**4.0266E7±0.22%**	**28.58**	**0.805**
TRIPOLI-4_B6_IRDF90 Next to inside of tank	**1.8031E7±0.25%**	**28.58**	**0.820**

Table B-2

****** this value is given by TRIPOLI-4 with a Watt spectrum between 15MeV and 1keV and parameters a = 1.012 and b = 2.249.**

Note the very similar values of the equivalent phosphorus fission flux densities given by the two evaluations for both measurement locations.

We shall therefore adopt this second method (equation 6bis) for evaluating the coefficient R_2. We shall use the IRDF_90 evaluations for calculating the equivalent phosphorus, rhodium and sulphur fission flux densities, and therefore use the following value for the coefficient R_2:

R_2 = 0.815 ±0.01

POINT D changing from the detector coefficient of the P31(n,p) dosimeter to those of S32(n,p), Ni58(n,p) and Rh103(n,n')

All these dosimeters are calibrated in NAÏADE 1 in a spectrum that is very close to but not strictly identical with the U235 fission spectrum. Allowance is made for this in the formalism leading to equation (7) of paragraph IV-7. To ensure that the dosimeters to be calibrated are irradiated homogenously, they are mounted on a rotating wheel. We are not aware of the precise position of the wheel: it is either in front of the outer surface of the aluminium tank (position (A) after the converter and before the tank), or next to the inner surface (position (B) of the tank on the void side) (see part D). Position B seems more likely for reasons of accessibility to the wheel. We repeated the calculation of the spectrum factors for the different dosimeters using the Monte Carlo program TRIPOLI-4 [9] for both of the possible wheel locations. The experimental set-up (described in part A) was modelled rigorously, as described in the forthcoming sections (parts C and D), the experimental void being empty. The spectrum factors with respect to P31 and the components $R_{3,K}$ (K = Rh103, S32) of the correction factors due to the fact that the spectrum is not strictly a fission spectrum at the calibration location, are given here:

	Rh103 Position A	**Rh103 Position B**	**S 32 Position A**	**S 32 Position B**	**Ni 58 Position A**	**Ni 58 Position B**
Ref. [3]	**1.375**		**0.98 ±0.02**		**0.964**	
TRIPOLI-4 + IRDF	**1.340**	**1.403**	**0.987**	**0.987**	**1.002**	**1.001**
R_3	**1.00±0.03**		**1.00±0.02**		**1.04±0.01**	

Table B-3

To conclude, the overall reassessment factors to be applied to the measurements made in the NAÏADE 1 assembly expressed in conventional flux densities are brought together in Table B-4 below. These values take account of all the factors identified.

Equivalent Mn and Mn/Cd (n,γ) thermal flux densities	**1.00**
Epithermal Au/Cd and In/Cd (n,γ) flux densities per unit of lethargy	**1.016**
Equivalent Rh103(n,n') fission flux densities	**0.815±0.04**
Equivalent S32(n,p) fission flux densities	**0.815±0.03**
Equivalent Ni58(n,p) fission flux densities	**0.848±0.02**
Equivalent P31(n,p) fission flux densities	**0.815±0.01**

Table B-4

It is important to note that these are systematic factors and that the uncertainties shown include only those arising from the location or counting of the dosimeters.

PART C

I Determining the power of the converter: the story

In this section we shall define the power of the NAÏADE 1 assembly plate and summarise the results of the basic measurements within the experimental area. All the results given in the different reports are normalised to a ZOE core power of 100kW, "in other words, a given value of the thermal flux escaping from the ZOE reflector" (reference condition). This thermal flux "is measured by a boron carbide γ-compensated ionisation chamber (C.C.P.N.10). The ionisation chamber is placed just before the cadmium-brass shutter, on the remaining graphite in the thermal column (20 cm below the bottom of the 60 cm diaphragm). Because of the possibility that the chamber or the current integration device might drift or fail completely, the current integration signals are linked to the output of manganese detectors placed on rod 2" (on the axis of the assembly about 2 cm in front of the uranium plate) in a configuration comprising the plate and boral diaphragm (diameter 60 cm) with the cadmium shutter raised. The stability of the chamber over time was investigated over a period from 30 June 1964 to 29 July 1965 by comparing the current and voltage it supplied with the equivalent manganese thermal flux density measured at the centre of rod 2. For the same voltage measured across a resistor (or current by counting the number of pulses), a scatter of 0.48% (0.64% on current) was found over 8 manganese measurements (was it the same dosimeter?). These measurements taken from reference [1] are set out in table C-1 below:

Dates	Mn flux density in terms of number of reference pulses x 1E7	Mn flux density in terms of reference voltage x 1E7
30-6-1964	**9.40**	**9.60**
24-12-1964	**10.7**	**10.7**
13-1-1965	**10.7**	**10.5**
14-5-1965	**9.43**	**9.59**
24-5-1965	**8.96**	**9.37**
9-6-1965	**9.57**	**9.57**
15-6-1965	**9.48**	**9.56**
29-7-1965	**9.40**	**9.52**

Table C-1

On 28 October 1958, the authors had checked the linearity of the chamber as a function of ZOE power between 10kW and 125kW. The scatter in the ratio of the number of pulses and the voltage is 1.9%. This scatter is deduced from table C-2 hereunder which is itself taken from reference [1].

ZOE power kW	Pulses/ Voltage Ratio
10	**2.19**
20	**2.17**
30	**2.26**
40	**2.25**
50	**2.19**
60	**2.20**
70	**2.16**
80	**2.16**
90	**2.18**
100	**2.28**
110	**2.28**
120	**2.23**
125	**2.23**

Table C-2

The linearity was checked again in 1964 from 100W to 15kW with scatter on the flux density values renormalized to 100kW of 3.7% as shown in table C-3 hereunder:

Dates	ZOE power levels	Flux densities renormalised to 100kW 1.E8
9-9-64	**150kW**	**1.09**
7-7-64	**100kW**	**1.05**
9-9-64	**30kW**	**1.00**
9-9-64	**10kW**	**1.06**
9-9-64	**3kW**	**1.10**
8-9-64	**1kW**	**1.00**
30-6-64	**500W**	**1.04**
8-9-64	**300W**	**1.04**
9-9-64	**100W**	**1.12**

Table C-3

Here is another relevant quotation from reference [1] about the precision of renormalisation: "with the cadmium shutter, the irradiation periods can be very precisely known (±1s). The accuracy of the renormalisation process stems from the precision of the current measurements using the integration system. Since the experiments were carried out with ZOE power levels ranging from 1 to 100kW, the precision of renormalisation is less than 1% when the two measurements are made close together in time, otherwise it depends upon the system stability over time, i.e., ±5%." (see tables above). As regards reactor control, we quote: "since most of the experiments done involved irradiating detectors, it was necessary to have the reactor power as stable as possible … the cadmium control rod is located in the central channel of ZOE and does not affect the flux density at the outlet from the thermal column. The observed stability is $\Delta P/P = 0.5\%$.

Finally we shall define the power of the plate in the reference conditions.
Analytical calculations using the collision by collision method (using the exponential integrals E1 and E2) and then diffusion theory (less precise) were carried out in August 1957 [10] by P. Lafore, J.P. Millot and J. Rastoin using one-group theory. These authors calculated that the converter behaved like an infinitely thin disc emitting $3.8^{E}7$ (±10%) neutrons/ cm^2.s in an isotropic manner for a ZOE power of 100kW. For each incident thermal neutron the fast flux density emitted towards the void was 0.588 and that towards the reactor, 0.631.

In 1967 [11], C. Fiche, G. Manent and P. Pépin did a calculation in spherical geometry using the SIDEF Monte Carlo program. Here the converter is regarded as a hollow sphere of radius 1m and thickness 2 cm, the inside being a notional substance with a very high inelastic effective cross-section (10000b/at), the outside being the void. These calculations **disagree, with their spectrum factor of R = 1.168** (Rh103/P31) with the more official but more recent publication [3] by J. Brisbois, M. Lott and G. Manent (R = 1.375) which we have adopted.

Calculations of the plate power were repeated in 1970 by M. Lott *et al* [1] using the following equation to determine the power of the plate:

$$P = \nu \times \Sigma_f \times \int_0^2 \phi_{th}(x)dx$$

In this equation the thermal neutron flux density was measured within the two centimetres of the natural uranium plate. The plate was in fact made up of 10 discs of uranium 2 mm thick with a manganese dosimeter positioned between each pair. The authors found $P = 5.0^{E}7$ fission neutrons/ cm^2.s for a ZOE power of 100kW. The flux density at the outlet from the plate on the void side was calculated using a Monte Carlo method.

We repeated these calculations for the converter power using the recent Monte Carlo program TRIPOLI-4. This will be described in part D. Paragraph II gives the results of the measurements done in 1964 which made our TRIPOLI-4 calculation possible.

II As-measures data from the measurements carried out in Naïade 1 within the experimental area

For recalculating the power of the plate, we have at our disposal a fine spatial distribution of the equivalent manganese thermal flux density in front of the converter. These neutrons are perfectly thermalised at ambient temperature; the cadmium ratio (R_{Cd}) exceeds 5000 ($R_{Cd} = Mn_{nu}/Mn_{/Cd}$). This makes it possible to determine the thermal neutron flux density incident on the plate as a function of the distance from its centreline. We also have measurements of the equivalent P31 fission flux density after the converter and measurements of the same parameter in the empty void. Comparison of these measurements with the results of the calculation will be one way of checking the calculated plate power. The results of the measurements carried out in NAÏADE 1 and reported in December 1970 in reference [1] are given in tables C-4 to C-7 below. Not all the measurements have been re-evaluated and are normalised in these tables to a reference ZOE power of 100kW.

Z cm	30-6-64	30-6-64	16-9-64	Z cm	30-6-64	30-6-64	16-9-64
39			**2.88E6**	**-5**	**9.60E7**	**9.60E7**	
37			**5.12E6**	**-10**	**9.60E7**	**9.60E7**	**9.52E7**
35			**9.58E6**	**-15**	**9.48E7**	**9.47E7**	
34			**1.33E7**	**-20**	**9.24E7**	**9.12E7**	**9.32E7**
33			**2.02E7**	**-25**	**8.36E7**	**8.05E7**	**8.68E7**
32			**5.42E7**	**-26**			**8.34E7**
31			**7.89E7**	**-27**			**8.00E7**
30	**8.29E7**	**8.15E7**	**8.25E7**	**-28**			**7.82E7**
29			**8.05E7**	**-29**			**7.73E7**
28			**8.43E7**	**-30**	**2.75E7**	**2.75E7**	**6.48E7**
27			**8.31E7**	**-31**			**5.24E7**
26			**8.76E7**	**-32**			**3.52E7**
25	**8.86E7**	**8.84E7**	**9.00E7**	**-33**			**2.20E7**
20	**9.23E7**	**9.28E7**	**9.36E7**	**-34**			**1.38E7**
15	**9.48E7**	**9.52E7**		**-35**			**1.14E7**
10	**9.60E7**	**9.60E7**	**9.60E7**	**-37**			**8.20E6**
5	**9.60E7**	**9.60E7**		**-39**			**5.61E6**
0	**9.60E7**	**9.60E7**	**9.60E7**				

Table C-4

Table C-4 shows all the flux densities equivalent to 2200m/s measured by the manganese dosimeters with, as indicated above, the cadmium ratio exceeding 5000. Three irradiation campaigns were done: two on 30 June 1964 and another, more comprehensive, on 16 September 1964. The measurement location is rod 2 (about 1.5 to 1.3 cm in front of the hot surface of the uranium plate); the dimension Z is measured from the centre of the converter. The spread of the results, where there are 3 of these for a given altitude Z will be used with table C-8 to analyse the scatter in the measurements in the absence of any flux density gradient and hence no uncertainty on the dosimeter location.

Z cm	2-6-1964	Z cm	2-6-1964
46.5	**3.67E6**	**-13.5**	**2.15E7**
36.5	**8.50E6**	**-23.5**	**1.74E7**
31.5	**1.22E7**	**28.5**	**1.36E7**
26.5	**1.57E7**	**-33.5**	**1.04E7**
21.5	**1.87E7**	**-38.5**	**7.10E6**
16.5	**2.05E7**	**-43.5**	**4.95E6**
-3.5	**2.20E7**	**-48.5**	**3.41E6**

Table C-5

Table C-5 gives the equivalent phosphorus (P31/Cd) fission flux density on the inner surface of the aluminium tank (at the so-called "zero tank" position, the origin of the abscissa x) which is 9 cm from the cold surface of the uranium plate, excluding the cladding. We may note the value that is practically on the centreline of the converter (Z = -3.5 cm): 2.20E7.

Z cm	2-6-1964	Z cm	2-6-1964
46.5	**5.05E6**	**-23.5**	**4.32E7**
36.5	**1.56E7**	**-28.5**	**3.02E7**
31.5	**2.88E7**	**-33.5**	**1.77E7**
26.5	**4.02E7**	**-38.5**	**1.02E7**
-3.5	**5.00E7**	**-43.5**	**5.63E6**
-13.5	**4.83E7**	**-48.5**	**3.58E6**

Table C-6

Table C-6 will be important for validating the estimated power of the fissile plate: it sets out the measurements made on 2 June 1964, expressed as equivalent phosphorus (P31/Cd) fission flux density on rod 1, in other words 2.6 cm behind the cold surface of the uranium plate. We may note the value on the centreline (owing to the low gradient, the measurement at Z = -3.5 cm can be regarded as being on the axis) of 5.00E7n. $cm^{-2}.s^{-1}$ expressed as fission neutrons. This value of 5.00E7 was used to determine the correction R_2 (table B-2).

Dist X cm	2-6-1964	Dist X cm	2-6-1964
0.0	**2.21E7**	**41.6**	**4.64E4**
7.5	**1.59E7**	**53.3**	**3.36E6**
13	**1.22E7**	**73.9**	**2.06E6**
18.6	**9.36E6**	**95**	**1.52E6**
24.5	**8.03E6**	**115**	**1.12E6**
32	**6.32E6**	**136**	**8.52E5**

Table C-7

Table C-7 shows the variation in the equivalent phosphorus fission flux density in the empty void and on the horizontal axis of the converter. The origin of the abscissa x is, as we have pointed out, the inner surface of the aluminium tank (in other words, on the void side). We shall use the value of 2.21E7 on the converter axis which we used for calculating the correction coefficient R_2 (table B-2).

Distance Z cm	1st measurement	2nd measurement	3rd measurement
30	**1.00729**	**0.99028**	**1.00243**
25	**0.99550**	**0.99326**	**1.01124**
20	**0.99354**	**0.99892**	**1.00754**
10	**1.00000**	**1.00000**	**1.00000**
0	**1.00000**	**1.00000**	**1.00000**
-10	**1.00279**	**1.00279**	**0.99443**
--20	**1.00145**	**0.98844**	**1.01011**
--25	**0.99960**	**0.96253**	**1.03786**

Table C-8

Table C-8 (not provided by those doing the measurements) has been deduced from table C-4 (values of the equivalent bare Mn thermal flux incident on the plate). On each line we have shown the ratio to the mean of the three measurements carried out at the same distance Z found in the three successive irradiations where these were done. We used the distances for which the vertical flux gradient was negligible or low such that there was no uncertainty on location. This approach excludes the three measurements at the distance -30 cm which in any event were unusual. The scatter in the ratios was calculated as 1.219%. We can therefore estimate the dispersion arising from the use of various manganese dosimeters as 1.2%, linked to the fact that the irradiation level fluctuated between the two measurements done in June and September 1964 respectively.

Other interesting measurements with the beam diameter set at 60 cm are given in reference [1]. They are shown here without our correction factors being applied and remain normalised to the ZOE power of 100kW.

Table C-9 shows the results of the measurements done on the centreline of the assembly **in the presence of the fissile plate and the boral screen, with the void empty.**

Measurement point	date	Measured flux	result
X=-12.4 on the axis	**30/06/64**	**Equivalent Mn thermal**	**9.60E7**
Front surface U plate	**24/05/65**	**Equivalent Mn thermal**	**9.60E7**
Rear surface U plate	**24/05/65**	**Equivalent Mn thermal**	**2.22E7**
X=-6.4 on axis	**02/06/64**	**P31 fission**	**5.00E7**
Internal tank surface x=0	**02/06/64**	**P31 fission**	**2.21E7**

Table C-9

Other measurements carried out, **this time without either the fissile plate or the boral screen,** can be used to analyse the background noise created by the fast and intermediate neutrons emanating from the ZOE core. These measurements are shown in table C-10 below

N	Position	date	Flux measured	Result
1	**On tank at (0; 0; 0)**	**26/05/65**	**Equivalent thermal Mn**	**6.40E7**
2	**On tank at (0; 0; 0)**	**26/05/65**	**Equivalent BF3/Cd thermal**	**5.41E3**
3	**On tank at (0; 0; 0)**	**25/05/65**	**Equivalent Mn/Cd thermal**	**9.90E3**
4	**On tank at (0; 0; 0)**	**25/05/65**	**Per unit of lethargy In/Cd (1.44eV)**	**1.71E4**
5	**On tank at (0; 0; 0)**	**24/05/65**	**Per unit of lethargy Au/Cd (4.91eV)**	**1.23E4**
6	**On tank at (0; 0; 0)**	**24/05/65**	**Equivalent S/Cd fission**	**6.35E4**
7	**On tank at (0; 0; 0)**	**25/05/65**	**Equivalent P/Cd fission**	**5.28E4**

Table C-10

On the next three pages we reproduce pages 48, 49 and 50 of reference [1] giving the background measurements in the empty NAÏADE 1 void, with the fissile plate and the boral screen once again in place.

STUDY WITH NAÏADE 1 EMPTY
BACKGROUND MEASUREMENTS

SOURCE: fission neutrons
DIAMETER: 60 cm
POWER: 5.107.n/cm2/s
Bare Mn: flux equivalent to v=2200m.s-1

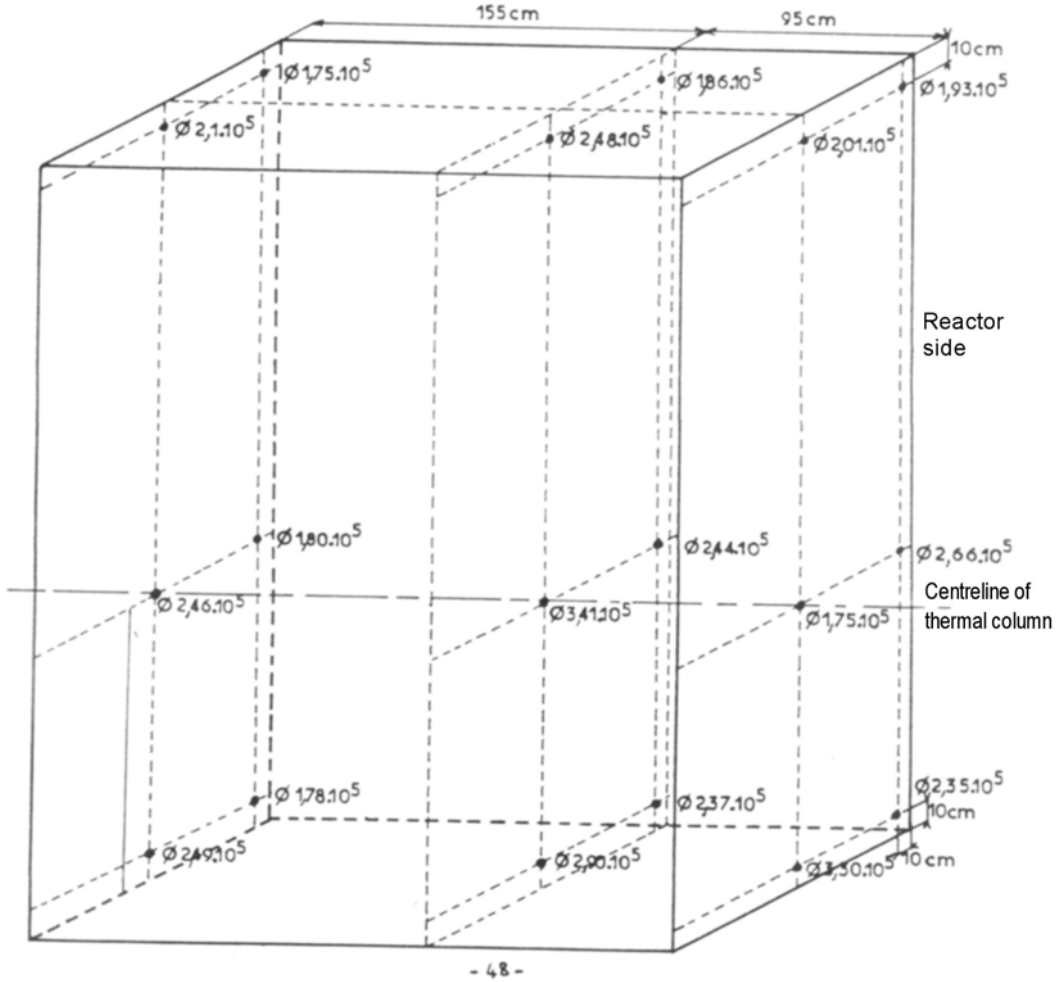

STUDY WITH NAÏADE 1 EMPTY
BACKGROUND MEASUREMENTS

SOURCE: fission neutrons
DIAMETER: 60 cm
POWER: 5.107.n/cm2/s
In/Cd: ø per unit of lethargy at 1.46eV
Mn/Cd: ø per unit of lethargy at 1.46eV

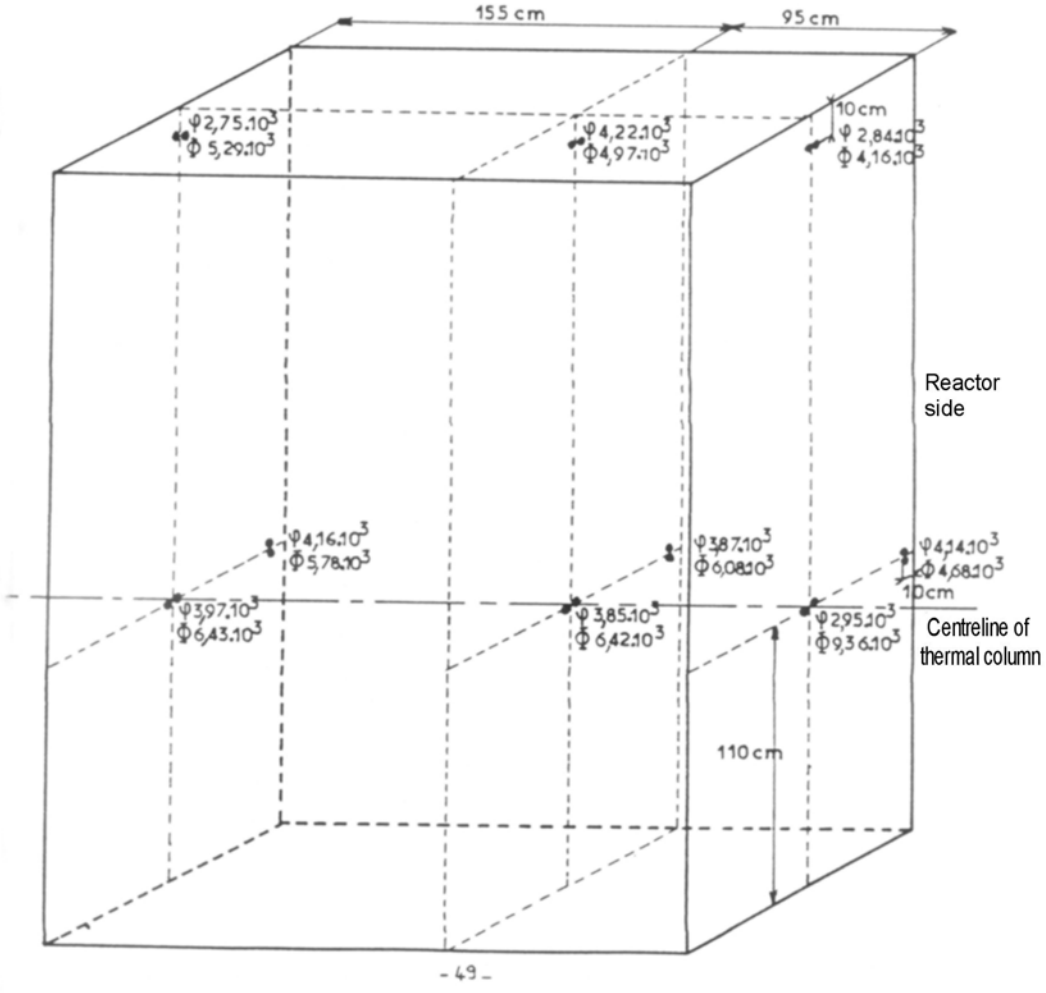

STUDY WITH NAÏADE 1 EMPTY
BACKGROUND MEASUREMENTS

SOURCE: fission neutrons
DIAMETER: 60 cm
POWER: 5.107.n/cm2/s
P/Cd: equivalent fission ø

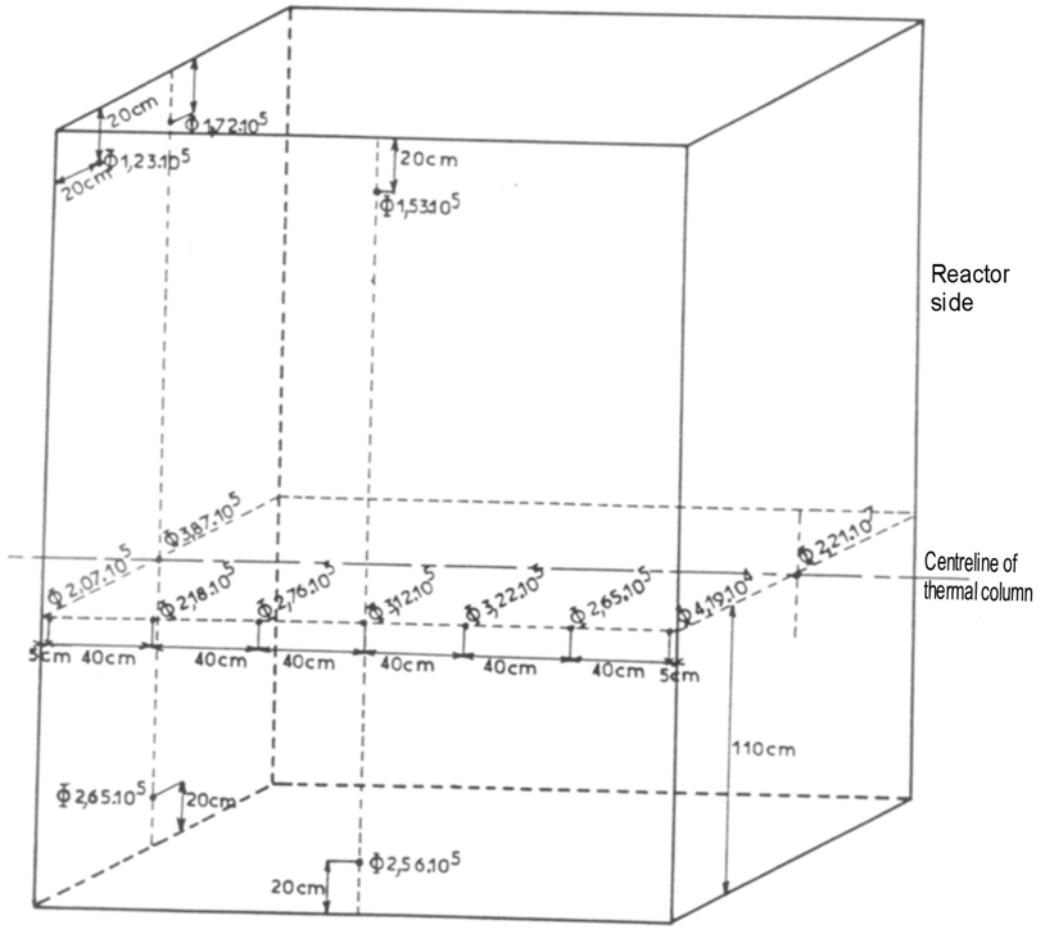

- 50 -

PART D

I CALCULATION OF THE CONVERTER POWER USING TRIPOLI-4 (2004): PRINCIPLES

The equivalent manganese thermal flux measured near the hot surface of the fissile plate is the sum of two terms:

1. The current of incident thermal neutrons coming directly from the graphite of the ZOE reflector,
2. The flux of thermal neutrons reflected from the plate itself and the structures in the vicinity of this plate.

First of all we set up a neutron current with a Maxwellian energy distribution to be incident on the plate so as to produce the equivalent thermal flux measured close to the hot surface of the converter (rod 1). Then, we did calculations using the TRIPOLI-4 program, with the NAÏADE 1 void still empty, with two objectives:

1. To obtain equivalent P31 fission fluxes so as to validate our model by comparisons with the fast neutron measurements.
2. To obtain Rh103/P31, Ni58/P31 and S32/P31 spectrum factors that are essential for resolving the question of the point D of part B (values given in table B-3)

The Fontenay-aux-Roses uranium plate has two original features that slightly complicate the interpretation of conventional flux measurements in the NAÏADE 1 void when it is empty and, particularly, when it contains a mock-up:

1. The plate is thick (2 cm), so multiple diffusions are possible;
2. It consists of natural uranium, so the fast neutrons resulting from fissions produced by thermal neutrons on U^{235} in turn produce fast fissions on U^{238}.

The boral plate situated after the converter in order to trap neutrons that are back-scattered from the mock-up is effective only against thermal neutrons, so that the few rare back-scattered intermediate or fast neutrons can induce fissions in the converter. These instances of back- scattering depend upon the type of mock-up placed in the void. They are few in number but not negligible even when the void is empty (about a tenth of one per cent).

The system consisting of converter + structures + mock-up **must therefore be treated as a subcritical system with a source of thermal neutrons;** the latter produce the first generation of fission neutrons (the most significant) which in turn produces successive generations that slightly amplify the power of the fissile plate.

The system was studied using the three-dimensional TRIPOLI-4 Monte Carlo program [9] the details of which are given hereunder.

	Calculations done at Saclay (Plate power)	**Other calculations (done by the author)**
Version	**v 4.3**	**v 4.3**
identification	**v 9.42 04/12/2001**	**v 9.55 28/11/2003**
T4 library	**1-1-11**	**1-1-11**
Geom library	**1-2_3**	**1-2-3**
Cplus library	**1-1-2**	**1-1-2**
Njoy library	**1-1-0**	**1-1-0**
Ipc library	**1-1-2**	**1-1-2**
hostname	**Is105587**	**Nimal1 and Nimal2**
Operating system	**Linux Red Hat 8.0**	**Linux Mandrake 9.2*[12]**

Table D-1

* except libstdc++-libc6.1-2.so.3 which comes from Linux Mandrake 7.2

There are two possible ways of interpreting the experiments carried out on NAÏADE 1 with due allowance for secondary fissions in the converter:

1. Starting with a source calculation that sets up a Maxwellian flux of thermal neutrons incident on the plate, and then calculating the density of first generation fission neutrons. Next, using the previously calculated fission sources, a subcritical source calculation is done with the mock-up present and the experiments interpreted using this latter calculation. For reasons of simplicity, one is then forced to accept that the radial distribution (along the radius of the uranium disc) of the flux of neutrons arising from the fissions is proportional to the incident thermal flux (no diffusion).
2. To handle the problem entirely as a single subcritical source calculation, the sources imposed being the incident thermal flux coming from ZOE, the mock-up being present in the simulation. This method is more stringent than the other (comprehensive treatment of the system). However this second method requires, for reasons of bias, the "MONITORING 0 **" option of TRIPOLI-4 to be used: this makes the choice of weighting parameters more difficult in circumstances where the void contains a mock-up. This second method was used for the situation where weighting is not necessary (the so-called "natural" simulation). This is the very interesting case where the NAÏADE 1 void is empty. It was also used in the situation in which the void is filled with light water (easy weighting).

** The MONITORING option of TRIPOLI-4 is used to correct the imperfections in the values of the bias parameters given by the user by adjusting the size of the population of simulated particles. MONITORING 0 eliminates this adjustment of the bias parameters. MONITORING cannot be used when a source of thermal neutrons is imposed which, absorbed by the boral, never reach the mock-up for which the results are sought.

II Model used for the TRIPOLI-4 calculations

II-1 Geometry

The geometry is described in three dimensions, the origin of the system of axes O being the intersection of the horizontal axis of the converter X'X and the surface of the aluminium tank on the void side. For x>0 the empty void is surrounded by parallelepiped blocks of ordinary concrete. For x<0 we have the converter assembly and the aluminium tank (-2 <x <0 cm). The different components are shown on figure D-1 hereunder.

In the experimental zone (x>0) two cylinders of axis X'X and respective radii of 5 and 10 cm are used to obtain reaction rates where they are intersected by planes perpendicular to the axis X'X. The conventional fluxes are deduced from these reaction rates. A technique for calculating the point wise value of the fluxes was also used.

In the zone containing the converter (x<0), three sets of volumes were used for obtaining average results. Starting from the ZOE side:

- **-12.6<x<-12.4** this part is broken down into discrete discs to obtain the equivalent Mn thermal flux (Volumes 8, 7, 6, 110, 5, 11, 112 and 113).
- **-11<x<-9** containing two square plates of natural uranium 100 cm along the side and 1 cm thick (volumes 11 and 12).
- **-6.5<x<-6.3** this part is broken down into discrete discs for obtaining the equivalent thermal fluxes (Mn) and equivalent P31 fission fluxes (volumes 19, 18, 17, 114, 16, 115, 15 and 116).

A volume denoted 1000 occasionally exists in the description of the geometry and hence in certain data files. It lies between the planes x=-240 and x=-25.8. Where it exists, it contains the necessary sources for calculating the background noise.

The atomic densities of the different materials used in our calculations are given in table D-2. The uniform composition of the boral is taken from reference [13 page 329]. This may be open to discussion.

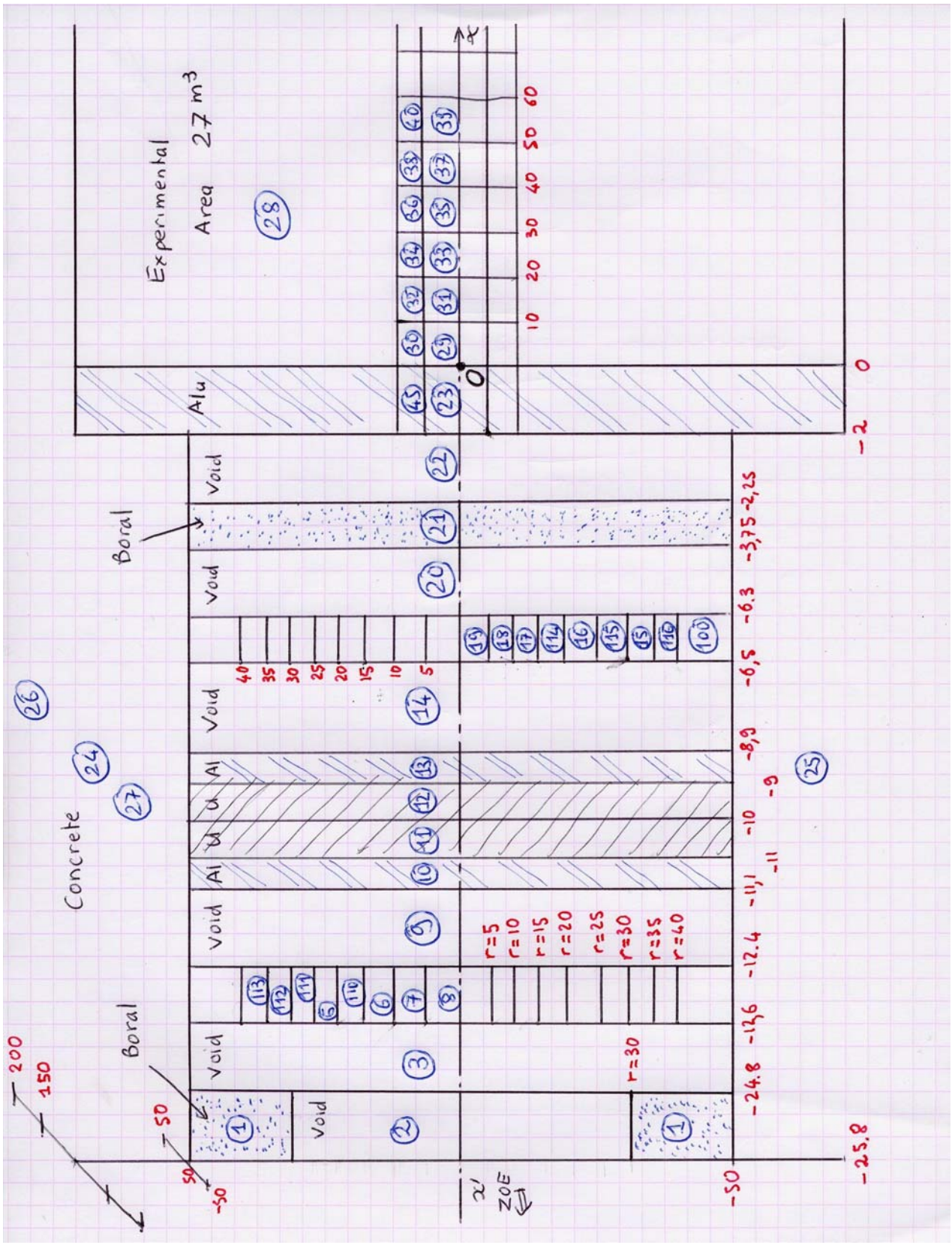
Experimental
Area 27 m3
Alu
Boral
Void
Concrete
Boral
Void
Void
Void
Al
Al
Al
Void
Void
Void
r=5
r=10
r=15
r=20
r=25
r=30
r=35
r=40
r=30
200
150
50
-50
50
-50
-2
0
-3,75
-2,25
-6,3
-6,5
-8,9
-9
-10
-11
-11,1
-12,4
-13,6
-24,8
-25,8
-50
Z'
ZOE
Y

boral	**Al27**	**4.518E-2**
boral	**C**	**5.456E-3**
boral	**B10**	**4.4037E-3**
boral	**B11**	**1.7726E-2**
aluminium	**Al27**	**6.0246E-2**
plate	**U235**	**3.4524E-4**
plate	**U238**	**4.7605E-2**
air	**O16**	**1.1315E-5**
air	**N14**	**4.2566E-5**
concrete	**Si**	**1.662E-2**
concrete	**Fe54**	**2.014E-5**
concrete	**Fe56**	**3.188E-4**
concrete	**Fe57**	**7.467E-6**
concrete	**Fe58**	**1.007E-6**
concrete	**H1**	**1.385E-2**
concrete	**O16**	**4.580E-2**
concrete	**Al27**	**1.746E-3**
concrete	**Ca**	**1.511E-3**
concrete	**Na23**	**9.641E-4**
concrete	**K**	**5.669E-4**
water	**O16**	**3.3373E-2**
water	**H_H2O**	**6.6746E-2**

Table D-2
Atoms per 1.E-24cm^3

Water is included in this table because the same data file is used for the situation where the void is filled with water.

II-2 Spatial, energy and angular distributions of the neutron sources used

First, it is possible to postulate a current of thermal neutrons on the fissile plate and use this source to do two types of calculation:

1. A source calculation excluding multiplication, giving the density of neutrons produced by fission in the converter: this is the first generation of fissions (***problem 1***)
2. A source calculation including multiplication (the TRIPOLI-4 FIXED_SOURCE_CRITICALITY option). We shall then obtain the density of all generations of neutrons arising from fission (***problem 2***).

Secondly (and in the case of *problem 1*), using the source density for fission neutrons resulting from problem 1, it is possible to resolve a fission source problem with multiplication by fissions (the TRIPOLI-4 FIXED_SOURCE_CRITICALITY option) in the presence of the void and the mock-up it contains (***problem 3***). We should point out that this last Monte-Carlo calculation is much easier to do than that arising from problem 2 as regards the selection of bias parameters. In this case – and in this case only – it is then possible to use the default option of TRIPOLI-4 which modifies the weighting: the MONITORING option.

II-2.1 Thermal neutron sources and density of fission neutrons in the converter

The source of thermal neutrons is a volume of revolution about the axis X'X and consists of a disc 80 cm in diameter (in fact virtually all the neutrons are emitted from a disc 60 cm in diameter corresponding to the diameter of the diaphragm we decided to interpret). The thickness of the disc is 0.01 cm lying between the abscissas -12.52 and -12.51. Since the core of ZOE and its reflector are far off (250 cm) and the source disc is very close to the fissile plate we have assumed that the neutrons followed a monodirectional path along X'X (tests reported in an earlier reference

[6] where concentrated neutrons were emitted in a cone of maximum angle showed that the greatest influence on the plate was 1.2%). The spatial and energy distribution of the thermal neutron source is given by the following equation:

$$S(\rho, E) = \lambda \times F(\rho) \times M(E)$$

where M(E) is the Maxwell distribution of neutrons at 27°C, which was the temperature of the experiment:

$$M(E)dE = \frac{2\pi}{(\pi kT)^{3/2}} \times \exp\left(-\frac{E}{kT}\right) \times \sqrt{E} \times dE$$

F(ρ) is the relative variation in the thermal flux equivalent to 2200m/s measured by the manganese dosimeters (given in table D-3) and λ is the normalisation constant calculated after simulation of the assembly in order to determine the value of the equivalent Mn thermal flux at 2200m/s on the axis at the reference location, i.e., 9.60E7n.cm^{-2}.s^{-1} . The value of λ we found is: λ=80×4.4311E6 or 3.5449E8 for a thickness of 0.01 cm along X'X

F(ρ) in 40 intervals of 1 cm				
19.20	**19.20**	**19.20**	**19.20**	**19.20**
19.20	**19.20**	**19.20**	**19.20**	**19.20**
19.20	**19.20**	**19.20**	**19.20**	**19.20**
19.20	**19.20**	**19.20**	**19.20**	**19.20**
19.04	**19.04**	**18.81**	**18.81**	**18.51**
18.51	**17.03**	**17.03**	**16.43**	**16.43**
12.10	**12.10**	**5.33**	**5.33**	**2.18**
2.18	**1.38**	**1.38**	**0.90**	**0.90**

Table D-3

With these conditions, we obtain the following results for the power of the plate, the first three lines of results being the density of neutrons emitted at abscissas -11, -10 and -9 respectively, averaged over the entire plate (1m^2) and the last two lines the values integrated over 1 cm of half-plate.

- **For problem 1 (first generation in n/s) table D-4 :**

location	**U^{235}**	**σ %**	**U^{238}**	**σ %**
X=-11 cm per unit of volume	**1.5274E7**	**0.0083**	**4.3534E1**	**0.0084**
X=-10 cm per unit of volume	**8.0190E6**	**0.0101**	**2.3176E1**	**0.0100**
X=- 9 cm per unit of volume	**3.3478E6**	**0.0156**	**9.7554E0**	**0.0155**
Integrated volume 11	**1.14853E11**	**0.0032**	**3.29639E5**	**0.0031**
Integrated volume 12	**5.55488E10**	**0.0054**	**1.61170E5**	**0.0053**
TOTAL plate	**1.70402E11**		**4.90809E5**	

Table D-4

The total power of the plate, which is 1.70402E11n/s, is slightly higher than the power given in April 2000 [6], where the value was 1.653E11 n/s, owing to an improved adjustment of the radial distribution F(ρ) in the calculation given here.

- **For problem 2 (taking all generations together in n/s) table D-5 :**

Location	**U^{235}**	**σ %**	**U^{238}**	**σ %**
X=-11 cm per unit of volume	**1.5362E7**	**0.027**	**8.5959E5**	**0.021**
X=-10 cm per unit of volume	**8.0844E6**	**0.033**	**1.0308E6**	**0.062**
X=- 9 cm per unit of volume	**3.4149E6**	**0.049**	**6.7899E5**	**0.068**
Integrated volume 11	**1.15600E11**	**0.012**	**1.04734E10**	**0.035**
Integrated volume 12	**5.61542E10**	**0.019**	**8.81344E9**	**0.036**
TOTAL plate	**1.71744E11**		**1.92886E10**	

Table D-5

The total power of the plate reaches 1.91041E11n/s including 1.70402E11n/s for the first generation and 2.0639E10n/s for the following generations. The increase in neutrons is 12.11% made up of 11.32% of fission neutrons on U238 and 0.79% on U235.

II-2.2 Density of fission neutrons for problem 3

Using the results for first generation neutrons given in paragraph II 2 1, one can define the density of the primary fission source neutrons for a subsequent propagation calculation in the void regardless of whether this is empty or contains a mock-up. It is reasonable to assume that:

1. The density of the first generation sources does not depend on whether a mock-up is present in the void since problem 1 involves only the thermal neutrons, and any thermal neutrons back-scattered by the mock-up towards the converter are completely absorbed by the boral screen;
2. The spectrum of the neutrons emitted in the first generation is the pure thermal fission spectrum of U235 (see table D-4).

The relevant constants for the source phase of TRIPOLI-4 are defined hereunder: they are all given in relative terms, since the source integral is fixed at 1.70402E11n/s, the value deduced from table D-4. The distribution at abscissa x (-11<x<-9) is given in table D-7:
These values are the result of measurements of thermal neutron flux obtained by stacking 20 discs of metallic natural uranium 0.1 cm in thickness, with a manganese dosimeter inserted between each disc. Figure D-7 ter shows a plot of these results.

X cm	Equivalent Mn55 thermal flux	X cm	Equivalent Mn55 thermal flux
-11.0	**3.58E7**	**-9.9**	**1.92E7**
-10.9	**3.50E7**	**-9.8**	**1.79E7**
-10.8	**3.37E7**	**-9.7**	**1.66E7**
-10.7	**3.2E7**	**-9.6**	**1.54E7**
-10.6	**3.01E7**	**-9.5**	**1.41E7**
-10.5	**2.84E7**	**-9.4**	**1.31E7**
-10.4	**2.67E7**	**-9.3**	**1.21E7**
-10.3	**2.51E7**	**-9.2**	**1.13E7**
-10.2	**2.37E7**	**-9.1**	**1.07E7**
-10.1	**2.21E7**	**-9.0**	**1.00E7**
-10.0	**2.07E7**		

Table D-7

Normalising the values in table D-7 from the power standpoint raises a problem: the value of the equivalent Mn55 thermal flux at x=-11 cm (which is 3.58E7) is very different from the value of 9.60E7 that might have been expected (ratio R=2.68).
The values of fission rate given in tables D-4 and D-5 are averaged (lines 2; 3; 4) or integrated (lines 5 and 6) over the entire surface A of the fissile plate, or 1.0E4cm^2. From these values of fission rate, it is possible to deduce:

- Mean values of equivalent U235 thermal fission flux (values used: υ=2.416 n/fission, N_5=3.4524E-4 atoms/ 10^{-24}cm^3, fission cross-section of 235 at 2200m/s=586.2b).
- And similar values on the fissile plate by assuming a flattening factor on the equivalent U235 thermal flux equal to the flattening factor F of the equivalent Mn55 thermal flux. The latter is obtained from table D-3 using the following equation:

$$F = \frac{F(0)}{\frac{1}{A}\int_0^{R\max} F(\rho) \times 2\pi\rho d\rho} \quad = 3.1408$$

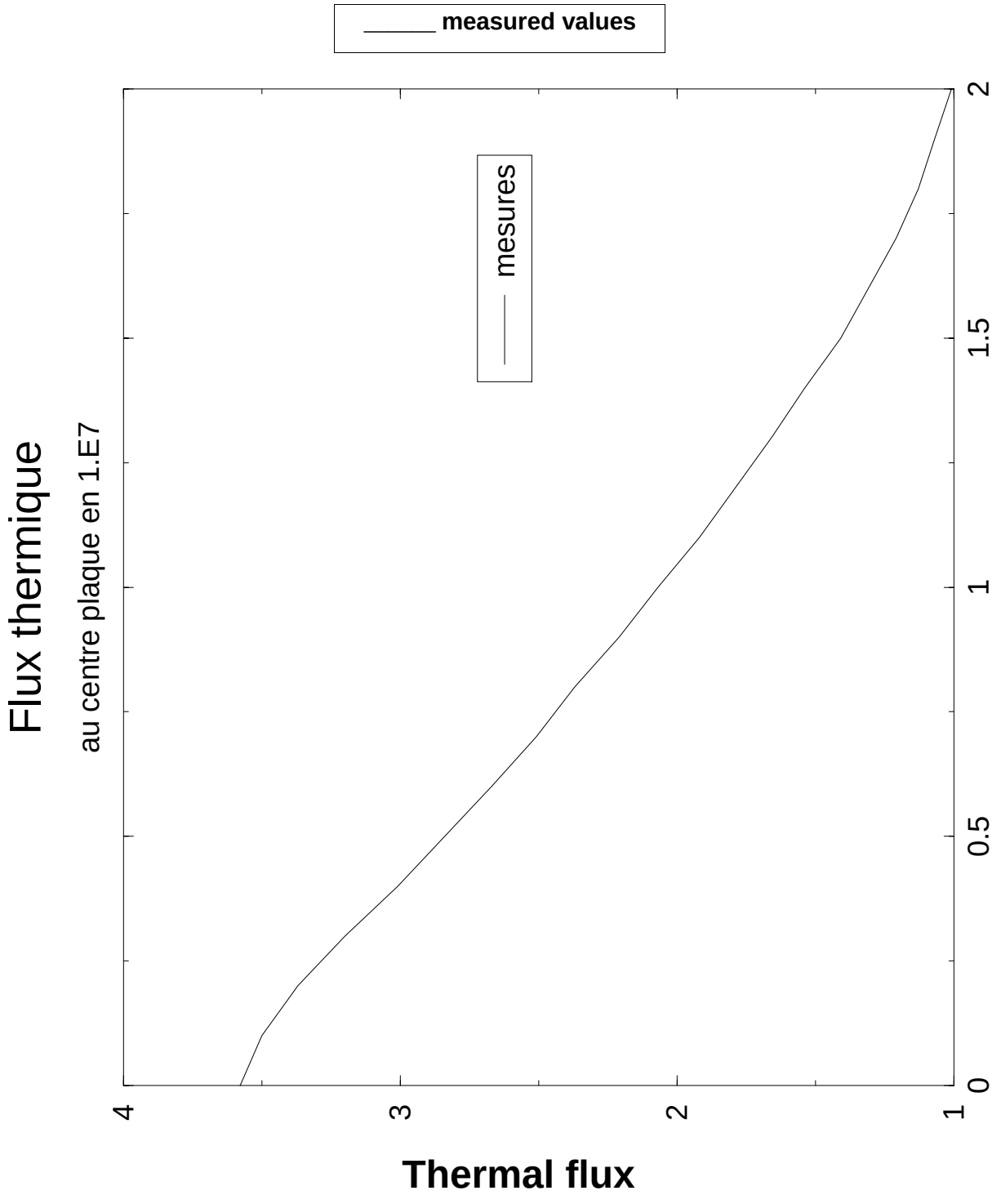

Figure D-7 ter
(not normalised)

The comparison along the axis of the converter of the calculated equivalent U235 thermal fluxes and the experimental equivalent Mn55 thermal fluxes normalised to 9.60E7 at x=-11 cm (R=2.68) is given in table D-7 bis below. Figure D-7-ter shows the plot of the measured thermal flux.

X cm	Equivalent U235 thermal flux TRIPOLI-4	Experimental equivalent Mn55 thermal flux
-11.0	**9.80E7**	**9.60E7**
-10.5	**7.41E7**	**7.61E7**
-10.0	**5.18E7**	**5.54E7**
-9.5	**3.61E7**	**3.78E7**
-9.0	**2.20E7**	**2.68E7**

Table D-7 bis

The radial distribution according to the variable ρ is taken from table D-3 although this represents a slight approximation: it is assumed that the fission density according to ρ is proportional to the incident thermal flux. This assumption is not made in resolving problem 2. The sources are emitted isotropically and we have adopted the Watt fission spectrum between 15MeV and 1keV with the parameters a=1.012 and b=2.249.

It is recalled that this source distribution can be used for interpreting any experiment on NAÏADE 1 so long as the TRIPOLI-4 FIXED_SOURCE_CRITICALITY option is imposed.

II-3 Neutron cross-sections used

The cross-sections used for the propagation calculation in the different materials are taken from ENDF/B-VI R4. They are employed in the point mode used by TRIPOLI-4 for a temperature of 300°K. Different response functions were used for phosphorous and manganese; when expressed in terms of conventional fluxes the results are the same but the reaction rates differ. For evaluating the power of the fissile plate we used the following:

P31(n,p)	IRDF_90	σ_f=0.02858b	recalculated*
Mn55(n,γ)	ENDF/B-VI/R4	σ_0=13.45b	[8]

For determining the background noise, we also employed the following evaluations:

S32(n,p)	IRDF_90	σ_f=0.06524b	recalculated*
Au197(n,γ)	IRDF_90	I=1565b	[8]
In115(n,γ)	ENDF/B-VI R4	I=3281b	[8]
Rh103(n,n')	IRDF_90	σ_f=0.7033b	recalculated*
B10(n,α)	ENDF/B-VI/R4	σ_0=3840b	[8]

* Watt fission spectrum a=1.012, b=2.249

III Comparisons between the TRIPOLI-4 calculations and measurements in the empty NAÏADE 1

All the calculations were done using the assumptions of problem 2 (see part D §II) with an incident source of thermal neutrons with fission multiplication (the FIXED_SOURCE_CRITICALITY option)

III-1 Equivalent Mn55 thermal flux

Tables D-9, D-10 and D-11 and the graph D-9 bis give in turn:

1. The equivalent Mn55 thermal flux at abscissa x=-12.4 cm for rings at different radii (D-9). The curve D-9 bis gives a comparison of the experimental values and those calculated by TRIPOLI-4 (step curve). The experimental results are measured along a vertical axis passing through the point (-12.4, 0, 0)
2. The equivalent Mn55 thermal flux at abscissa -6.4 cm (D-10) made up solely of neutrons passing through the fissile plate.

3. The equivalent Mn55 thermal flux of neutrons returning towards the ZOE core after reflection at the converter and the neighbouring structures (D-11).

ρ	Reaction rate	Standard deviation %	Mn55 thermal flux
0 to 5	**1.2833E9**	**0.061**	**9.541E7 EXP=9.60E7**
5 to 10	**1.2824E9**	**0.035**	**9.536E7**
10 to 15	**1.2803E9**	**0.027**	**9.519E7**
15 to 20	**1.2761E9**	**0.030**	**9.488E7**
20 to 25	**1.2430E9**	**0.019**	**9.242E7**
25 to 30	**1.1107E9**	**0.018**	**8.258E7**
30 to 35	**4.9703E8**	**0.029**	**3.695E7**
35 to 40	**1.1274E8**	**0.096**	**8.382E6**

Table D-9

ρ	Reaction rate	Standard deviation %	Mn55 thermal flux
0 to 5	**2.7800E8**	**0.106**	**2.067E7 EXP=2.22E7**
5 to 10	**2.7686E8**	**0.063**	**2.058E7**
10 to 15	**2.7591E8**	**0.047**	**2.051E7**
15 to 20	**2.7317E8**	**0.040**	**2.031E7**
20 to 25	**2.6265E8**	**0.035**	**1.953E7**
25 to 30	**2.2883E8**	**0.034**	**1.701E7**
30 to 35	**1.1064E8**	**0.048**	**0.833E7**
35 to 40	**3.1864E7**	**0.112**	**0.237E7**

Table D-10

ρ	Reaction rate	Standard deviation %	Mn55 thermal flux
0 to 5	**2.4988E8**	**0.19**	**1.858E7**
5 to 10	**2.4820E8**	**0.11**	**1.845E7**
10 to 15	**2.4616E8**	**0.082**	**1.830E7**
15 to 20	**2.4128E8**	**0.072**	**1.794E7**
20 to 25	**2.2799E8**	**0.065**	**1.695E7**
25 to 30	**1.9063E8**	**0.062**	**1.417E7**
30 to 35	**1.0736E8**	**0.090**	**7.982E6**
35 to 40	**4.2746E7**	**0.17**	**3.178E6**

Table D-11

III-2 Equivalent phosphorous P31 fission flux

All the equivalent fission fluxes given **in this paragraph have been corrected** as indicated in table B-4. Table D-12 and graph D-12 bis give the mean values of equivalent fission fluxes in small rings lying in a plane at abscissa -6.4 cm.

ρ	Reaction rate	Standard deviation %	P31 fission flux
0 to 5	**1.1508E6**	**0.17**	**4.027E7 EXP=4.075E7**
5 to 10	**1.1356E6**	**0.097**	**3.973E7**
10 to 15	**1.1110E6**	**0.076**	**3.887E7**
15 to 20	**1.0646E6**	**0.063**	**3.725E7**
20 to 25	**9.6982E5**	**0.06**	**3.393E7**
25 to 30	**7.8725E5**	**0.059**	**2.755E7**
30 to 35	**5.0429E5**	**0.073**	**1.764E7**
35 to 40	**2.6280E5**	**0.11**	**0.920E7**

Table D-12

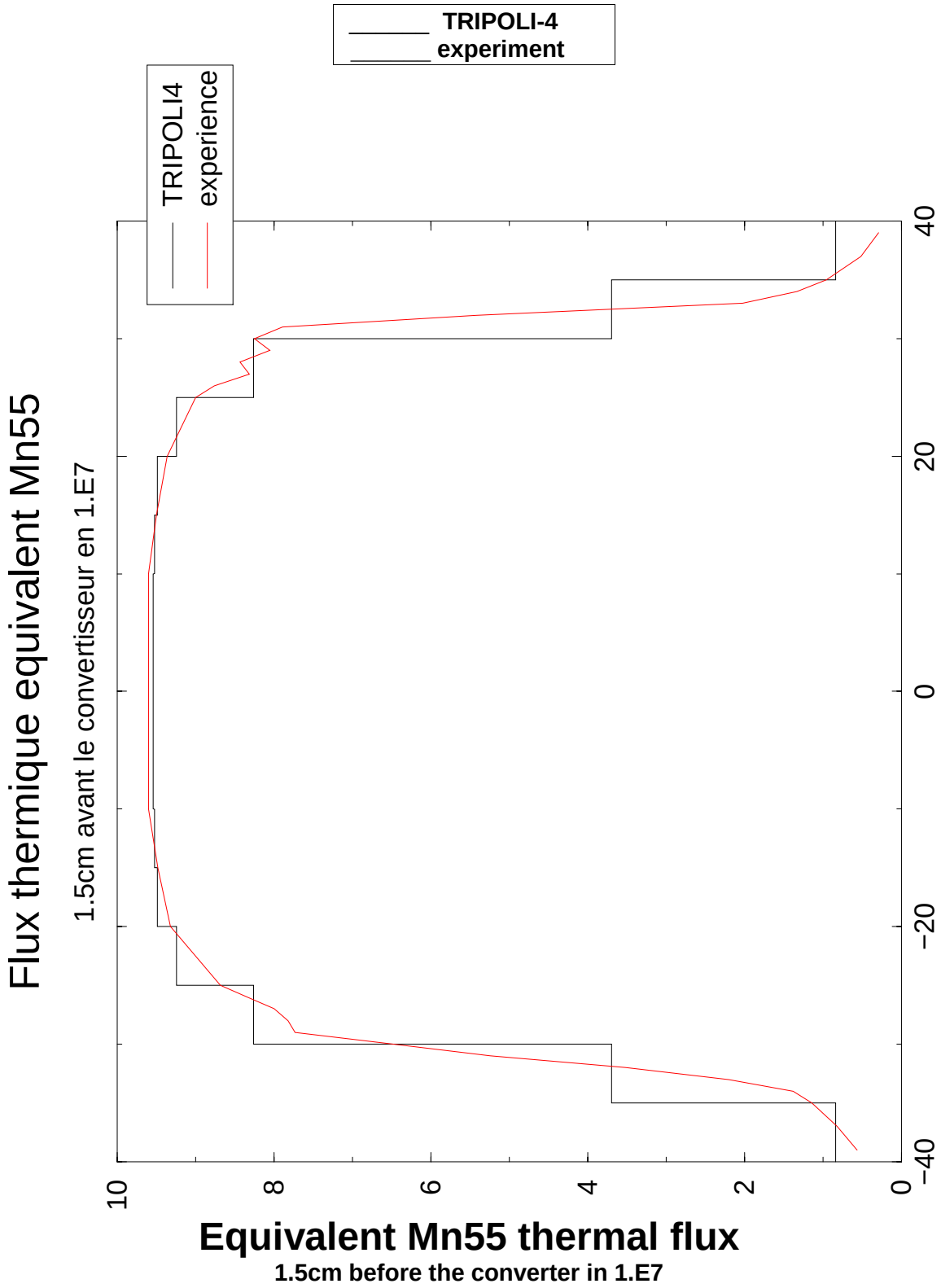

Figure D-9 bis

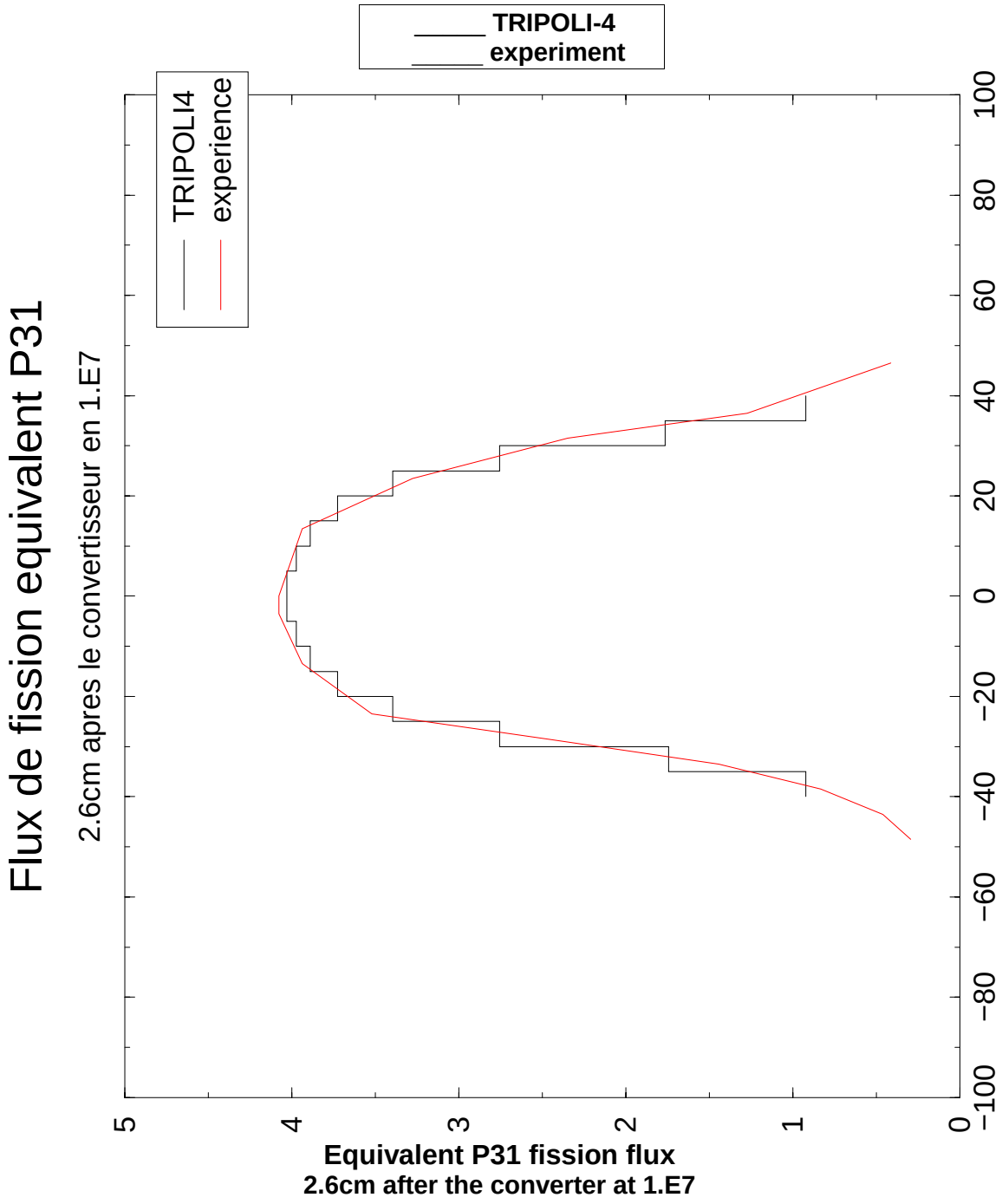

Figure D-12 bis

Because of the importance of these equivalent phosphorous P31 fission fluxes in checking the power of the fissile plate, we employed the point estimator of TRIPOLI-4 using the technique assuming that every neutron follows an impact-free path after each collision with a nucleus (FXPT option). Table D-13 shows the values calculated by TRIPOLI-4 together with the experimental values in the plane x =-6.4 cm (after the fissile plate).

Distance z cm	Reaction rate	Standard deviation %	TRIPOLI-4 fission flux	Experiment (corrected)	C/E
-3.5	1.1475E6	0.27	4.015E7	4.075E7	0.985
-13.5	1.1051E6	0.27	3.867E7	3.936E7	0.982
-23.5	9.4302E5	0.29	3.300E7	3.520E7	0.937
-28.5	7.4667E5	0.36	2.613E7	2.461E7	1.061
-33.5	4.4387E »5	0.41	1.553E7	1.443E7	1.077
-38.5	2.2792E5	0.45	7.975E6	8.313E6	0.959
-43.5	1.2400E5	0.57	4.339E6	4.588E6	0.946
-48.5	7.7735E4	0.58	2.720E6	2.918E6	0.932
+26.5	8.3999E5	0.31	2.939E7	3.276E7	0.897
+91.5	5.6874E2	0.36	1.990E7	2.347E7	0.848
+36.5	2.9969E5	0.40	1.049E7	1.190E7	0.831

Table D-13

A check point was located at x=0.1, y=0, z=0 (practically next to the inner surface of the aluminium tank). The TRIPOLI-4 calculation gives an equivalent phosphorous fission flux of 1.771E7 (±0.49%) while the measurement shows 1.793E7 (C/E=0.988).

A second series of results for the equivalent phosphorous fission flux is given in table D-14 and reproduced on the graph D-14 bis: these are comparisons of the values in the empty NAÏADE 1 void on the axis of the converter. The calculations are obtained either by using mean values on the discs of radius 5 cm (SURF) or using the technique of the point estimator (FXPT) for the larger distances. At long distances, the presence of background noise can be observed, certainly due to neutrons coming from the ZOE core.

Technique	X cm	Reaction rate	Standard deviation %	TRIPOLI-4 P31 flux	Measured P31 flux (corrected)	C/E
SURF	0.0	5.1707E5	0.46	1.809E7	1.801E7	1.004
SURF	7.5	3.6699E5	0.37	1.284E7	1.296E7	0.991
SURF	13.0	2.8823E5	0.40	1.009E7	0.994E7	1.014
SURF	18.6	2.2774E5	0.43	7.969E6	7.628E6	1.045
SURF	24.5	1.7907E5	0.49	6.266E6	6.544E6	0.957
SURF	32.0	1.3708E5	0.55	4.796E6	5.151E6	0.931
SURF	41.6	1.0137E5	0.62	3.547E6	3.782E6	0.938
FXPT	53.3	7.1938E4	0.25	2.517E6	2.738E6	0.919
FXPT	73.9	4.4525E4	0.32	1.558E6	1.679E6	0.928
FXPT	95.0	2.9746E4	0.37	1.041E6	1.239E6	0.840
FXPT	115.0	2.1694E4	0.40	7.591E5	9.128E5	0.832
FXPT	136.0	1.6550E4	0.46	5.791E5	7.025E5	0.824

Table D-14

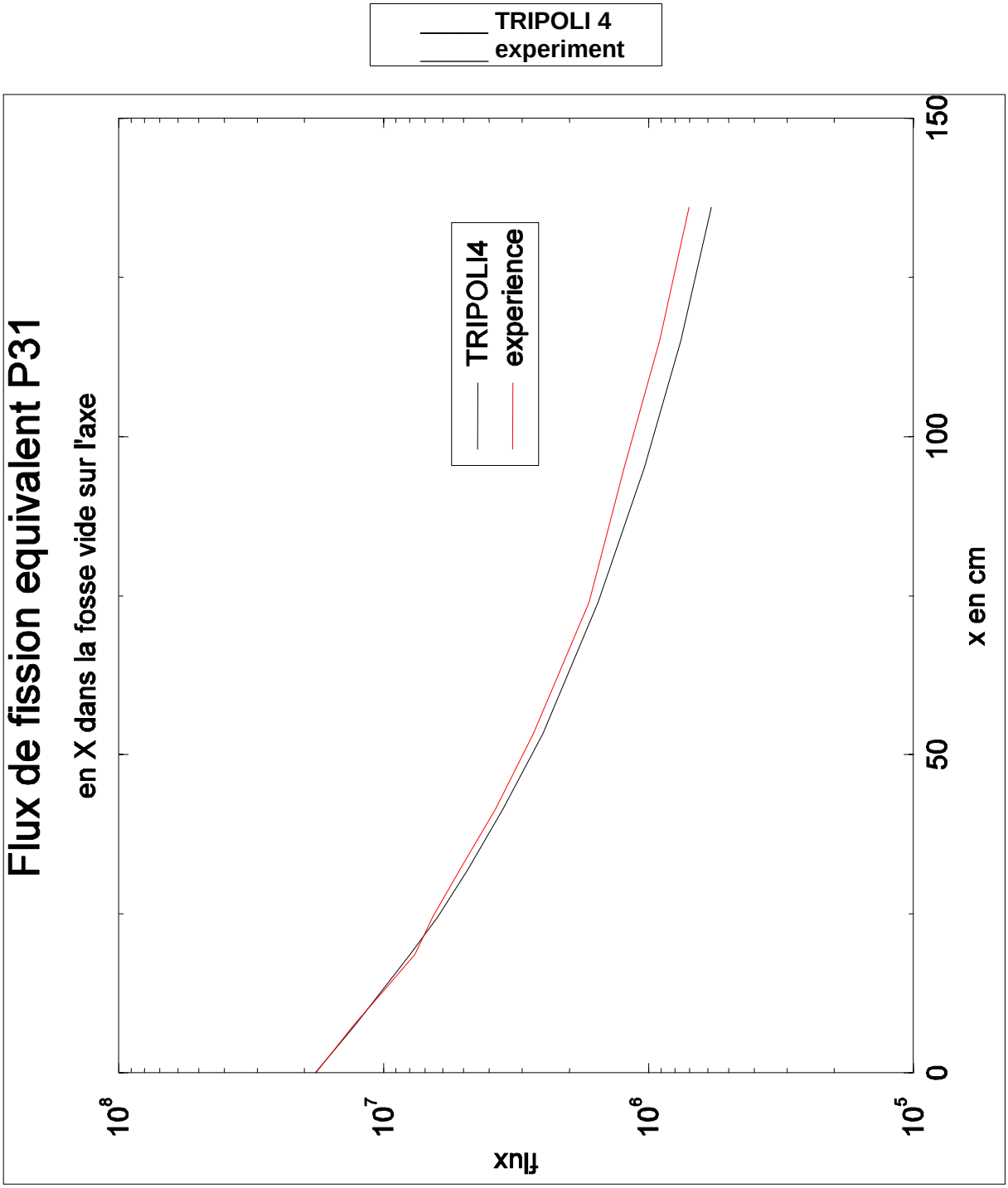

Equivalent P31 fission flux
at X in the empty void on the axis

Figure D-14 bis

IV The problem of background noise

IV-1 Presence of background noise

Despite all the precautions taken to eliminate background noise, a small proportion of the fast and intermediate neutrons emanating from the ZOE core manages to pass through the different shields (heavy water and graphite reflector). These neutrons are an unwanted addition to the thermalised neutrons irradiating the converter: they pass through it and the boral screen and cause slight interference with the measurements made in the mock-ups positioned in the NAÏADE 1 experimental area.
Allowance must also be made for:

- (γ,n) reactions in mock-ups containing light elements (for example, water with high penetration).
- Photo-fission reactions on the fission chambers which have been used for different experiments.

To the best of my knowledge, no measurements have been made of photon spectra in NAÏADE 1 nor have neutron-photon calculations been done in the mock-ups.

However as regards background noise due to fast and intermediate neutrons, measurements [1] were done in May 1965 in the following conditions:

- Natural uranium plate absent
- Boral screen absent
- Diaphragm diameter 60 cm
- Tank in position
- ZOE power set at 100kW

Table D-15, taken from reference [1], gives the measured and corrected data (see table B-4) from which the neutron background noise on the axis of the converter on the inner surface of the aluminium tank (x = 0, y = 0, z = 0) can be estimated.

Dosimeter	Unit	Measured value	Corrected value
Bare Mn55	**Equivalent thermal flux**	**6.40E7**	**6.40E7**
BF3/Cd	**Equivalent thermal flux**	**5.41E3**	**5.41E3**
Mn55/Cd	**Equivalent thermal flux**	**9.90E3**	**9.90E3**
In115/Cd	**Flux/lethargy unit 1.46eV**	**1.71E4**	**1.74E4**
Au197/Cd	**Flux /lethargy unit 4.91eV**	**1.23E4**	**1.25E4**
S32	**Equivalent fission flux**	**6.35E4**	**5.18E4**
P31	**Equivalent fission flux**	**5.28E4**	**4.30E4**

Table D-15

It will be seen that the fast neutron background noise (P31) reaches 0.24% at the inner surface of the aluminium tank because the measured value with the complete converter is 2.20E7. This relative value will increase with distance in the void because the geometrical attenuation is greater for the fast neutrons emanating from the converter than for those emanating from the ZOE core

IV-2 Estimating the source of background noise

Using the values for conventional flux given in table D-15, a TRIPOLI-4 calculation was used to determine what the flux would have been in the absence of the aluminium tank with a spectrum model made up first of a fission spectrum and, secondly, of a constant spectrum per unit of lethargy between 0.1MeV and 0.5eV. A ZOE source is then modelled which reproduces this composite spectrum at the origin of the axis and the void.

We created an isotropic point source at abscissa -230 cm centred on the converter axis with intensity $\mathbf{S_{noise}(E)}$ given by the following equation:

$$\mathbf{S_{noise}(E) = (S_f(E))\times 2.54E9 + 6.61E8/E \ \ n/s\times steradian\times MeV}$$

Where $S_F(E)$ designates the fission spectrum of U235 due to thermal neutrons and where the 1/E portion is applied only between 0.1MeV and 0.5eV.

Two Monte Carlo calculations were done using the TRIPOLI-4 program: the first (table D-16) included all the structures except for the fissile plate and the boral screen, while the other (table D-17) showing how the equivalent phosphorus fission flux changes in the empty NAÏADE 1 void, assumes the fissile plate and the boral screen to be in position.

dosimeter	unit	TRIPOLI-4 + model	Corrected experiment	C/E
Bare Mn55	**Equivalent thermal flux**		**6.40E7**	
BF3/Cd	**Equivalent thermal flux**	**6.15E3**	**5.41E3**	**1.14**
Mn55/Cd	**Equivalent thermal flux**	**1.23E4**	**9.90E3**	**1.24**
In115/Cd	**Flux / lethargy unit 1.46eV**	**1.35E4**	**1.74E4**	**0.78**
Au197/Cd	**Flux / lethargy unit 4.91eV**	**1.35E4**	**1.25E4**	**1.08**
S32	**Equivalent fission flux**	**4.79E4**	**5.18E4**	**0.92**
P31	**Equivalent fission flux**	**4.83E4**	**4.30E4**	**1.12**

Table D-16

technique	X cm	Noise reaction rate	Standard deviation %	TRIPOLI-4 P31 flux signal	TRIPOLI-4 P31 flux noise	Noise/Signal in %
SURF	**0.0**	**9.777E2**	**0.89**	**1.809E7**	**3.421E4**	**0.19**
SURF	**7.5**	**8.784E2**	**0.78**	**1.284E7**	**3.073E4**	**0.24**
SURF	**13.0**	**8.143E2**	**0.79**	**1.009E7**	**2.849E4**	**0.28**
SURF	**18.6**	**7.526E2**	**0.80**	**7.969E6**	**2.633E4**	**0.33**
SURF	**24.5**	**6.933E2**	**0.85**	**6.266E6**	**2.426E4**	**0.39**
SURF	**32.0**	**6.422E2**	**0.88**	**4.796E6**	**2.247E4**	**0.47**
SURF	**41.6**		**0.**	**3.547E6**		
FXPT	**53.3**	**5.044E2**	**0.075**	**2.517E6**	**1.765E4**	**0.70**
FXPT	**73.9**	**4.143E2**	**0.085**	**1.558E6**	**1.450E4**	**0.93**
FXPT	**95.0**	**3.462E2**	**0.086**	**1.041E6**	**1.211E4**	**1.16**
FXPT	**115.0**	**2.978E2**	**0.090**	**7.591E5**	**1.042E4**	**1.37**
FXPT	**136.0**	**2.574E2**	**0.091**	**5.791E5**	**0.901E4**	**1.56**

Table D-17

V Conclusions

The above data (part D) can be used to interpret the different mock-ups placed in the NAÏADE 1 experimental area:

- Either using the fission density in the plate, the integral of which is 1.70402E11 n/s.
- Or using the Maxwellian thermal neutron flux given in § II-2-1

In both cases a subcritical source problem will have to be dealt with (FIXED_SOURCE_CRITICALITY) with proper adjustment of the bias parameters if the "MONITORING 0" option is used.

As regards the interpretation of experiments carried out during one and the same irradiation, the control stability reported by the experimenters is better than 0.5%. The authors indicate that the power settings for the different irradiations is better than 1% for those separated by a short period of time and within 5% for those at longer intervals. The spread we found (table C-8) in the measurements using bare manganese is 1.2% whereas we found the dispersion arising from the analysis at different powers (from 100W to 150kW) to be 3.7%. Although all these uncertainties are low, it is interesting to look more closely at experiments that were done during one and the same irradiation.

Owing to the fact that the cadmium shutter falls quickly (1s) the duration of the irradiations is extremely precise.

The correction we propose to make to the experimental values of conventional fluxes is known to within 5% (Rh103), 4% (S32) and 2% (P31).

All that remains is the uncertainty about the location of the dosimeters. The authors state that rods 1, 2 and 3 are positioned to within 2 mm which has no effect on the power of the converter. As regards the dosimeters placed in the mock-ups we shall examine – where these exist – different measurements at the same location made on different dates.

The major advantage of the NAÏADE 1 experiments is that the dosimeters were calibrated each with respect to the others, which ensures coherence.
As regards the background noise, we found that fast neutron noise reached 0.2% nearby and about 2% farther off. It seems to us that this value is underestimated when we consider the C/E values in table D-14 or curve D-14-bis as from a distance of 60 cm. This may be due to the contribution of multiple diffusions in the experimental area, imperfect knowledge of the composition of the boral (the experiments on iron support this postulate) or to the model used for calculating the background noise itself.

PART E

Experiments carried out on the iron block

I Description of the experiment on the iron block

The NAÏADE 1 assembly was described in part A of the present report. In the experiment in question, the experimental void contains an assembly of 30 plates of extra-mild steel, 5 cm in thickness and measuring 200 cm by 200 cm. The assembly thus forms a block measuring 200 cm × 200 cm × 150 cm, the thickness of 150 cm being located along the axis of the converter starting from abscissa 0 which is located at the inner surface of the aluminium tank. The plates are suspended from beams. The mock-up is surrounded by wooden boards except on the upper surface. The characteristics of the steel are given in reference [1]:

Specific gravity: 7.85 ±0.02
Carbon content: 0.15% by weight

In this experiment, the diaphragm diameter was 60 cm. A central hole of diameter 3 cm can be stopped up with steel plugs of various thicknesses (5 cm, 2 cm, 1 cm and 0.5 cm). The dosimeters to be irradiated are positioned between the plugs. The location of these dosimeters is known to within 0.1 cm [1 page 18] by measuring the distance from the dosimeter positioned at the end of the channel. The experiments were carried out between May and July 1963 and the results are reported in reference [1] in tables 10-1 to 10-3; the graphs of conventional flux attenuation are on figures PL10-1 (for fast neutrons) and PL10-2 (for the epithermal and thermal dosimeters).

II Raw data and corrected experimental results

The calibrated dosimeters (see part B) used in the 1963 experiments, the responses of which were interpreted using the TRIPOLI-4 Monte Carlo program, are listed hereunder:

1. P/Cd reaction - P31(n,p) - thickness 3 mm.
2. WIGNER Si based upon damage formation in a silicon diode 5 mm in diameter and 0.25 mm in thickness [14]. The response function used to convert the neutron spectrum directly to the equivalent Wigner fission flux is given in appendix 1. This is extracted from appendix V of reference [14]. We verified that the integral of this response function weighted by our fission spectrum was practically equally to unity since we found 0.9970 ± 0.0002.
3. Rh/Cd reaction - Rh103(n,n') - thickness 0.2 mm.
4. Np237/Cd fission chamber. As yet we have no data on the precision of the calibration of this chamber. If this was done behind the NAÏADE 1 plate, then a multiplication factor of 0.815 would have to be applied (see part B). We shall give both solutions, corrected and uncorrected by this factor.
5. Bare Mn and Mn clad in Cd. In fact the responses of the bare and cadmium-sheathed dosimeters expressed in thermal fluxes equivalent to 2200m/s are the same in iron. The difference calculated by TRIPOLI-4 is negligible in view of the statistical dispersion.
6. Ni/Cd: we have not interpreted the results of this dosimeter which are expressed in terms of equivalent **thermal** flux (Ni(n,γ)).
7. In/Cd reaction (n,γ) with a deposit of 0.1 mg/cm^2 giving fluxes per unit of lethargy.
8. Au/Cd reaction (n,γ) with a deposit of 0.1 mg/cm^2 giving fluxes per unit of lethargy.
9. Two fission chambers for thermal and epithermal neutrons were used by the experimental team and the results were interpreted using TRIPOLI-4: U235(n,f) and Pu239(n,f). We have not yet found any data on the calibration of the chambers. It seems likely that the calibration was done in the standard block in Fontenay-aux-Roses or by comparison with an equivalent thermal flux measured using a manganese dosimeter in a purely thermal spectrum. In these circumstances no correction would have to be applied to the measured equivalent thermal fluxes. However the chambers were located in a high gamma environment and it is likely that there were photo-fissions resulting from highly energetic photons coming from the capture of neutrons by the iron nuclei or directly from the ZOE core.
10. S32/Cd reaction (n,p). This dosimeter was not positioned in the iron block. Notwithstanding this we calculated the corresponding reaction rate so that it could be compared with the P31 (n,p) device of similar sensitivity.

The as-measured experimental results are considered together with the corrected experimental results (see part B §V) in paragraph III below. The correction factors for converting the basic experimental data into corrected results are summarised in the table below. As regards the activation dosimeters, these factors are obtained from part B; as concerns the fission chambers, we are unaware how they were calibrated, but this was probably using the standard block: we have therefore assumed a value of unity for the correction coefficient. As regards the equivalent WIGNER silicon fission flux, reference [14] sets out the procedures for calibrating silicon diodes. In principle this involves:

1. irradiating diodes in the presence of calibrated phosphorus dosimeters. This irradiation was done on rod 0 which was positioned next to the aluminium tank, in the NAÏADE 1 experimental area side, the latter being empty. The equivalent phosphorus fission flux was known - $\phi_P(1965)$.
2. multiplying the flux $\phi_P(1965)$ by the spectrum factor $R_{W/P}(1965)$ obtained by dividing the equivalent WIGNER silicon fission flux by the equivalent phosphorus fission flux. In 1965 this factor was calculated and a value of 1.22 found [14, page 14] for the spectrum behind the NAÏADE 1 aluminium tank.

These corrections were applied to all these calculations. As concerns the spectrum $R_{W/P}(2005)$ calculated by the TRIPOLI-4 program in the precise configuration of NAÏADE 1, we found 1.520 at the location of rod 0 on a disc of radius 5 cm. In a ring between the radii 5 and 10 cm we found $R_{W/P}(2005) = 1.529$ or a difference of 0.6%.

The overall correction factor for the WIGNER silicon equivalent fission flux is therefore the product of the correction factor on the equivalent phosphorus fission flux $\phi_P(2005)/ \phi_P(1965) = 0.815$ by the ratio $R_{W/P}(2005)/R_{W/P}(1965) = 1.52/1.22$. We therefore obtain for the equivalent WIGNER graphite fission flux a correction factor of 1.015 ±0.02.

Equivalent Mn and Mn/Cd thermal fluxes (n,γ)	**1.00**
Epithermal fluxes per unit of lethargy Au/Cd and In/Cd (n,γ)	**1.016**
Equivalent Rh103 fission flux (n,n')	**0.815±0.04**
Equivalent S32 fission flux (n,p)	**0.815±0.03**
Equivalent Np237 fission flux (n,f)	**0.815 or 1.00**
Equivalent P31 fission flux (n,p)	**0.815±0.01**
Thermal Equivalent U235 flux (n,f)	**1.00**
Thermal Equivalent Pu239 flux (n,f)	**1.00**
WIGNER Si equivalent fission flux	**1.015±0.02**

As far as the positioning of the dosimeters is concerned we can give the following uncertainty expressed in centimetres $\Delta x = \pm\left(0.1 + 2.5\times10^{-3}\times x\right)$

where the first term is the uncertainty on the measurements as estimated by the experimental team themselves, and the second term results from the uncertainty as to the density of the mild steel for an interpretation carried out with a specific gravity of 7.85.

As regards the uncertainties affecting the detection coefficient, the reproducibility of the power of the plate and the counting process itself, we shall use the values given in table E-1 below. When a measurement has been repeated and gives results R_1 and R_2, we calculated the difference $\varepsilon = 100(R_1/R_2 - 1)$ as a function of abscissa x and the type of dosimeter measured.

X cm	dosimeter	ε %
0	P/Cd	0.0
5.5	P/Cd	-4.2
11	P/Cd	-4.5
16.5	P/Cd	+6.6
22	P/Cd	-16
27.5	P/Cd	-5.6
33	P/Cd	-3.3
38.5	P/Cd	-10
0	Mn/Cd	-1.2
10	Mn/Cd	+3.4
16	Mn/Cd	-19
21	Mn/Cd	-13
37	Mn/Cd	-13
42	Mn/Cd	-8.7
15	Bare Mn	+4.2

Table E-1

The square route of the mean of the squares of the deviations is 9.3% on all the dosimeters with a slightly lower value for the fast neutron dosimeters (7.7%) and hence a higher value for the epithermal dosimeters (10.7%).

III As-measured results and interpretation by the TRIPOLI-4 program

All the experiments on the iron mock-up were interpreted using the TRIPOLI-4 Monte Carlo program [9]. The need to use the "MONITORING" option for this type of problem with difficult weighting (see part D § 1) forced us to solve the type 3 problem (see part D § II-2). We therefore use the sources of first generation fission neutrons in the converter 2 cm in thickness with the TRIPOLI-4 option "FIXED_SOURCE_CRITICALITY". It is recalled that the normalisation of the calculation is equal to 1.70402E11n/s emitted between 19.8MeV and 0.001MeV with a Watt spectrum for the thermal fission neutrons from U235 (a = 1.012 and b = 2.249).
Reference [1] stipulates that the wood surrounding the iron block consisted of boards. We assumed that this was poplar for which we obtained the composition from reference [15]. Table E-2 gives the composition of the iron mock-up partly surrounded by wood.

Iron	Atoms/10E-24cm^3
C	5.9047E-4
Fe54	4.9875E-3
Fe56	7.7534E-2
Fe57	1.7752E-3
Fe58	0.2367E-3
Wood	**Atoms/10E-24cm^3**
O16	0.00970
H_H2O (bound)	0.00602
H1 ("free")	0.01338
C	0.00803

Table E-2

Other composition data are given in paragraph II-1 of part D (table D-2).
In volume 28 (iron parallelepiped: 150 cm along x, 200 cm along y and 200 cm along z) we arranged a series of 55 cylindrical volumes iron (volumes 200 to 254) of radius 5 cm , axis Ox , bounded by planes perpendicular to that axis with abscissas x_K. This makes it possible to obtain mean values of reaction rates on discs of radius 5 cm at abscissas x_K. The volumes 528, 628 and 828 consist of wood.

The mean values on the fission spectrum σ_f, the resonance integral I and the effective cross-section at 2200m/s (σ_0) are given below. These are used to convert reaction rates to conventional fluxes; **they are coherent with the values of the neutron point cross-sections used in the calculation of reaction rates during the interpretation using the TRIPOLI-4 program.**

P31(n,p)	IRDF_90	σ_f=0.02858b	recalculated
Mn55(n,γ)	ENDF/B-VI/R4	σ_0=13.45b	[8]
S32(n,p)	IRDF_90	σ_f=0.06524b	recalculated
Au197(n,γ)	IRDF_90	I=1565b	[8]
In115(n,γ)	ENDF/B-VI R4	I=3281b	[8]
Rh103(n,n')	IRDF_90	σ_f=0.7033b	recalculated
Np237(n,f)	ENDF/B-VI R4	σ_f=1.305b	[8]
Si WIGNER	[14]	σ_f=0.9970	[14] after recalculation
U235(n,f)	ENDF/B-VI R4	σ_0=586.2b	[8]
Pu239(n,f)	ENDF/B-VI R4	σ_0=751.4b	[8]

The TRIPOLI-4 calculation (reference 04-030) of 15/12/2004 used the data file "naiadefer_2004.data" from the directory /home/nimal/TRIPOLI-4/NAIADE_FER/ of the nimal2 station and comprised 250 "batches" of 330000 neutrons. It required 690221s on a PC running at 2.7GHz.

The following table gives the number of fission neutrons per second resulting from first generation fissions. These are the second and subsequent generation fission neutrons obtained using the "FIXED_SOURCE_CRITICALITY" option:

location	U235	σ %	U238	σ %
1st cm of plate	**1.1503E9**	**0.092**	**1.0761E10**	**0.028**
2nd cm of plate	**1.0201E9**	**0.085**	**9.3448E9**	**0.028**
Total for plate	**2.1704E9**		**2.0106E10**	

The second and subsequent fission generations therefore contribute an additional converter power of 13.07%. The additional neutrons are emitted with their respective fission spectrum (U235 and U238) corresponding to the energy of the neutron that led to their emission.

The following tables show the experimental results and the results of the calculation done using the TRIPOLI-4 program expressed as conventional fluxes. The columns headed "rates" correspond to the microscopic reaction rates (the integral of the neutron cross-section in barns/atom weighted by the value of the neutron flux $cm^{-2}.s^{-1}.MeV^{-1}$). The columns headed "flux" correspond to the values of conventional flux. The symbol σ represents the statistical uncertainty on the calculated results due solely to the stochastic nature of the Monte Carlo method.

abscissa	S32 reaction rate	Standard deviation σ %	Equivalent S32 flux
0	**1.428E6**	**0.71**	**2.188E7**
5.5	**4.070E5**	**1.4**	**6.239E6**
11	**1.356E5**	**2.7**	**2.078E6**
16.5	**4.444E4**	**2.4**	**6.812E5**
22	**1.660E4**	**3.4**	**2.544E5**
27.5	**5.793E3**	**4.0**	**8.880E4**
33	**1.810E3**	**3.5**	**2.774E4**
38.5	**7.022E2**	**5.1**	**1.076E4**
44	**2.458E2**	**5.5**	**3.768E3**

Table E-3 (no experimental values)

abscissa	TRIPOLI-4 Calculated P31 rate	σ %	TRIPOLI-4 Calculated P31 rate	Raw Experimental data	Corrected experimental data	C/E
0	**6.447E5**	**0.69**	**2.255E7**	**2.50E7** **2.50E7**	**2.04E7** **2.04E7**	**1.11** **1.11**
5.5	**1.876E5**	**1.1**	**6.564E6**	**8.00E6** **8.35E6**	**6.52E6** **6.81E6**	**1.01** **0.96**
11	**6.374E4**	**2.1**	**2.230E6**	**2.94E6** **3.08E6**	**2.40E6** **2.51E6**	**0.93** **0.89**
16.5	**2.140E4**	**2.2**	**7.488E5**	**1.13E6** **1.06E6**	**9.25E5** **8.64E5**	**0.81** **0.87**
22	**8.131E3**	**2.9**	**2.845E5**	**3.85E5** **4.58E5**	**3.14E5** **3.73E5**	**0.91** **0.76**
27.5	**2.858E3**	**3.3**	**1.000E5**	**2.02E5** **2.14E5**	**1.64E5** **1.74E5**	**0.61** **0.57**
33	**9.383E2**	**3.0**	**3.283E4**	**1.17E5** **1.21E5**	**9.54E4** **9.86E4**	**0.34** **0.32**
38.5	**3.628E2**	**4.2**	**1.268E4**	**7.02E4** **7.80E4**	**5.72E4** **6.36E4**	**0.22** **0.20**
44	**1.332E2**	**5.4**	**4.661E3**	**4.06E4**	**3.31E4**	**0.14**

Table E-4

The first line of the raw experimental results corresponds to the measurements made on 15/03/1963, and the second line to those conducted on 21/05/1963. One partial conclusion can be drawn: the calculated equivalent phosphorus fission flux is attenuated much more quickly than the corresponding (mutually coherent) experimental values (an error factor 7 for an attenuation of a factor of about 300).

Table E-5 gives the results (equivalent WIGNER graphite) produced by the TRIPOLI-4 calculation and by the experiment.

X cm	TRIPOLI-4 Wigner rate	σ %	Experimental data
0	**5.892E7**	**0.25**	**8.87E7**
10	**2.244E7**	**0.22**	**2.31E7**
20	**1.047E7**	**0.22**	**1.20E7**
30	**5.335E6**	**0.19**	**5.00E6**
40	**2.881E6**	**0.20**	**3.12E6**
50	**1.616E6**	**0.18**	**1.75E6**
60	**9.335E5**	**0.26**	**9.65E5**
70	**5.484E5**	**0.20**	**5.15E5**
80	**3.281E5**	**0.22**	**3.12E5**
90	**2.000E5**	**0.69**	**2.52E4**

Table E-5 (As-measured WIGNER Si)

The calculation 05_002 we carried out shows that the response function $\sigma_W(E)$ given in appendix V of reference [14] and reproduced in our own appendix is virtually normalised to unity when it is weighted by the Watt fission spectrum of 235 (a = 1. 012 and b = 2.249). We have:

$$\int_0^\infty \sigma_W(E) s_f(E) dE = 0.9970$$

This is the value used to convert the "reaction rate" to the equivalent Wigner silicon fission flux from table E-5bis.

X cm	TRIPOLI-4 Wigner flux	σ %	Corrected experimental data	C/E
0	5.910E7	0.25	9.00E7	0.66
10	2.251E7	0.22	2.34E7	0.96
20	1.050E7	0.22	1.22E7	0.86
30	5.351E6	0.19	5.08E6	1.05
40	2.890E6	0.20	3.17E6	0.91
50	1.621E6	0.18	1.77E6	0.91
60	9.363E5	0.26	9.79E5	0.96
70	5.500E5	0.20	5.23E5	1.05
80	3.291E5	0.22	3.17E5	1.04
90	2.006E5	0.69	2.56E5	0.78

Table E-5bis (Corrected WIGNER Si)

X cm	TRIPOLI-4 Rh103 rate	TRIPOLI-4 Rh103 equiv flux	σ %	As-measured results	Corrected experimental data	C/E
0	3.019E7	4.294E7	0.32	4.56E7	3.72E7	1.15
10	8.788E6	1.250E7	0.34	1.62E7	1.32E7	0.95
20	3.255E6	4.630E6	0.34	5.79E6	4.72E6	0.98
30	1.379E6	1.962E6	0.32	2.29E6	1.87E6	1.05
40	6.428E5	9.144E5	0.29	1.12E6	9.13E5	1.00
60	1.701E5	2.420E5	0.26	4.48E5	3.65E5	0.66
80	5.301E4	7.541E4	0.24	9.63E4	7.85E4	0.96
100	1.835E4	2.610E4	0.29	4.27E4	3.48E4	0.75
120	6.786E3	9.653E3	0.22	1.094E4	8.92E3	1.08

Table E-6

The values of equivalent WIGNER Si and rhodium fission fluxes are coherent and acceptable.

X cm	TRIPOLI-4 Np237 rate	σ %	TRIPOLI-4 Np237 flux	As-measured results	C/E (1)	C/E (2)
0	6.170E7	0.31	4.728E7	3.50E7	1.35	1.10
5	3.268E7	0.33	2.504E7	2.34E7	1.07	0.87
10	1.892E7	0.33	1.450E7	1.25E7	1.16	0.95
15	1.135E7	0.36	8.700E6	9.08E6	0.96	0.78
20	7.005E6	0.36	5.368E6	4.56E6	1.18	0.96
25	4.433E6	0.36	3.397E6	2.60E6	1.31	1.07
35	1.909E6	0.30	1.463E6	1.39E6	1.05	0.86
45	8.938E5	0.28	6.849E5	5.98E5	1.15	0.94
55	4.462E5	0.29	3.419E5	2.63E5	1.30	1.06

Table E-7

The values of C/E in column (1) are the result of dividing the equivalent fission fluxes given by TRIPOLI-4 by the as-measured experimental values, while the values in column (2) are for the case in which the Np237 chamber is calibrated with respect to the fast neutron flux behind the NAÏADE 1 assembly the as-measured values of which are overestimated, as we have seen, by a factor 1/0.815

X cm	Exp 1	Exp 2	Exp 3	TRIPOLI Rate	σ %	Calculated flux	C/E
0	2.38E5	2.41E5		1.378E6	1.8	1.025E5	0.43
2.24	2.70E5			2.081E6	1.4	1.547E5	0.57
5.0	3.00E5			2.803E6	1.2	2.084E5	0.69
6.72	3.00E5			3.195E6	1.2	2.375E5	0.79
10.	3.34E5	3.23E5		3.705E6	1.0	2.755E5	0.84
16	2.76E5		3.40E5	4.038E6	1.0	3.002E5	0.97
21	2.58E5	2.95E5					
26.5	2.38E5			3.811E6	1.0	2.833E5	1.19
30		2.35E5		3.639E6	1.0	2.706E5	1.15
32.16	2.14E5			3.426E6	0.9	2.547E5	1.19
37	1.86E5	2.13E5	1.85E5	3.137E6	1.9	2.332E5	1.20
42	1.67E5	1.83E5		2.806E6	1.1	2.086E5	1.19
46.5		1.57E5		2.457E6	0.98	1.827E5	1.16
52.1		1.36E5		2.169E6	1	1.613E5	1.19
56.5			1.02E5	1.875E6	1.1	1.394E5	1.37

Table E-8 (initial comparisons relative to Mn/Cd)

The three columns headed Exp1, Exp2 and Exp3 correspond to the equivalent thermal fluxes at 2200m/s measured using the Mn/Cd dosimeters, the dates of the experiments being 15/05/1963, 20/05/1963 and 01/07/1963 respectively.

X cm	Exp 1	Exp 2	Exp3	TRIPOLI Rate	σ %	Calculated flux	C/E
62.0		1.14E5		1.620E6	1.1	1.204E5	1.06
67.5		8.03E4		1.372E6	1.1	1.020E5	1.27
73.04		6.94E4		1.159E6	1.1	8.617E4	1.24
77.0			5.85E4				
78.28		5.81E4		9.841E5	1.3	7.317E4	1.26
83.52		4.81E4		8.724E5	1.3	5.486E4	1.14
88.76		4.08E4		7.123E5	1.2	5.296E4	1.30
94.0		3.33E4		6.078E5	1.4	4.519E4	1.36
97.7			2.80E4				
99.24		3.15E4		4.961E5	1.6	3.688E4	1.17
104.48		2.53E4		4.231E5	1.4	3.146E4	1.24
110.0		2.00E4		3.641E5	2.2	2.707E4	1.35
118.3			1.32E4				
119.96		1.44E4		2.452E5	1.9	1.823E4	1.27
130.0		9.14E3		1.576E5	1.8	1.172E4	1.28
135.44		7.23E3		1.125E5	2.3	8.364E3	1.16
140.68		5.79E3		7.956E4	2.6	5.915E3	1.02
145.92		4.83E3		4.556E4	3.7	3.387E3	0.70

Table E-8 (Mn/Cd continued)

The proportion of the conventional flux located below the cadmium cut-off (0.5eV in the calculations) is 1% or less.

X cm	TRIPOLI Rate	σ %	TRIPOLI Flux	As-measured results	Corrected measurement data	C/E
0	3.815E7	3.4	1.163E4	5.00E4	5.08E4	0.23
5	1.306E8	4.3	3.980E4	6.54E4	6.64E4	0.60
10	2.025E5	3.4	6.172E4	9.10E4	9.24E4	0.67
20	3.053E8	9	9.305E4	1.08E5	1.10E5	0.85
30	2.558E8	2.7	7.796E4	8.70E4	8.84E4	0.88
40	2.333E8	2.9	7.111E4	7.50E4	7.62E4	0.93
50	1.734E8	3.0	5.282E4	3.40E4	3.45E4	1.53
60	1.414E8	3.9	4.310E4	4.73E4	4.81E4	0.90
70	1.006E8	3.0	3.066E4	2.86E4	2.91E4	1.06
80	8.008E7	5.5	2.441E4	1.99E4	2.02E4	1.21
90	5.663E7	3.4	1.726E4	1.74E4	1.77E4	0.98
110	2.804E7	3.8	8.546E3	7.25E3	7.37E3	1.16
130	1.228E7	4.4	3.743E3	3.77E3	3.83E3	0.98
150	(1.163E7)	72		1.72E3	1.75E3	(2)

Table E-9

Table E-9 gives the results of the calculations and of the measurements for indium in cadmium (resonance at 1.46eV)

X cm	TRIPOLI Rate	σ %	TRIPOLI flux	As-measured results	Corrected measurement data	C/E
0	3.916E7	5.2	2.502E4	7.07E4	7.18E4	0.35
5	1.449E8	3.3	9.259E4	1.62E5	1.65E5	0.56
10	2.306E8	8.1	1.473E5			
16	2.724E8	3.7	1.741E5	1.86E5	1.89E5	0.92
30	2.684E8	2.5	1.715E5	1.70E5	1.73E5	0.99
40	2.294E8	2.6	1.466E5			
46.5	2.021E8	3.1	1.291E5	1.24E5	1.26E5	1.02
50	1.827E8	2.7	1.167E5			
60	1.404E8	3.2	0.897E5			
62	1.312E8	2.9	8.383E4	8.15E4	8.28E4	1.01
67.5	1.134E8	2.9	7.246E4	5.89E4	5.98E4	1.21
70	1.051E8	2.8	6.716E4			
77	8.487E7	2.6	5.423E4	5.30E4	5.38E4	1.01
91.92	5.604E7	3.2	3.581E4	3.15E4	3.20E4	1.12
117.16	2.213E7	3.8	1.414E4	1.29E4	1.31E4	1.08
142.4	5.808E6	7.5	3.711E3	4.91E3	4.99E3	0.74

Table E-10

Table E-10 compares the conventional fluxes obtained from the calculations with the activation measurements using Au/Cd (resonance at 4.91eV)

X cm	TRIPOLI Rate	σ %	TRIPOLI flux	As-measured results	C/E
0	1.289E8	0.24	2.199E5	4.79E5	0.46
5	1.220E8	0.45	2.081E5	6.14E5	0.40
10	1.207E8	0.45	2.059E5	5.14E5	0.40
15	1.158E8	0.53	1.975E5	4.44E5	0.44
25	9.863E7	0.50	1.682E5	3.57E5	0.47
50	5.242E7	0.56	8.942E4	1.90E6	0.47
70	2.903E7	0.99	4.952E4	8.87E4	0.56

Table E-11

X cm	TRIPOLI Rate	σ %	TRIPOLI flux	As-measured results	C/E
0	**1.584E8**	**0.29**	**2.108E5**	**3.35E5**	**0.63**
10	**1.376E8**	**0.63**	**1.831E5**	**3.74E5**	**0.49**
20	**1.237E8**	**0.74**	**1.646E5**	**3.10E5**	**0.53**
30	**1.047E8**	**0.95**	**1.393E5**	**2.19E5**	**0.64**
50	**6.543E7**	**3.4**	**8.708E4**	**1.29E5**	**0.68**
80	**2.547E7**	**1.32**	**3.390E4**	**4.39E4**	**0.77**
110	**9.028E6**	**1.43**	**1.201E4**	**1.79E4**	**0.67**

Table E-12

Tables E-11 and E-12 bring together the results given by the fission chambers using U235 and Pu239 respectively. The TRIPOLI-4 flux is expressed in thermal equivalent flux at 2200m/s. Two interesting facts may be noted:

1. at present the documents setting out the process of calibrating these fission chambers are not in our hands.
2. we have carried out a rapid order of magnitude calculation which shows that the chambers are not perturbed by the photo-fissions resulting from gammas emanating from neutron capture in iron nuclei. To demonstrate this point, we evaluated the source of photons (and then the flux of photons) in a constant equivalent thermal flux and calculated the resulting photo fissions ($\sigma_{a,iron}$ = 2.56b, N_{iron} = 0.0846 at/ 10^{-24} cm^3, 59% of 8 MeV photons by capture, attenuation coefficient of iron for the 8 MeV gammas = 0.2319 cm^{-1}, photo-fission cross-section of U235 = 0.03b at 8MeV and fission cross-section of the neutrons at 2200m/s = 586.2b).

IV Background noise estimation using TRIPOLI-4 Code

A calculation of the background noise contribution due to the fast and epithermal neutrons (E > 0.5eV) stemming from the ZOE reactor core was made using the TRIPOLI-4 software. The Maxwellian thermal neutrons stemming from the ZOE's reflector cross the first uranium converter then are absorbed by the thick borated screen. The determination of the neutron source generating the background noise is presented in part D in front of the experiment descriptions.

Let us recall (see details in the table D-15) the levels of the experimental flux measurements under the following conditions:

1. Absence of the uranium converter carrying out the conversion of the thermal neutrons into fission neutrons
2. Absence of the thick borated screen
3. Diaphragm of 60cm
4. aluminium tank in place
5. ZOE's power equal to 100kW
6. Measurement in the axis of the converter on the internal face of the aluminium tank (x=y=z=0)

The experimental values of the neutron flux on the internal face of the tank are:

1. Thermal equivalent flux to 2200m / s 6.4E7
2. Flux by unity of lethargy 1.E4 to 2.E4
3. Equivalent fission flux 4.0E4 to 5.0E4

Let us also recall the order of the equivalent fission flux at the same point with, this time, the presence of the fission converter and the borated screen: 1.8E7

The results below are obtained with a source of background noise corresponding to that described in the paragraph IV-2 of part D. The neutrons are emitted only in a cone of axis Ox and from a vertex angle Arccos (0.95) to limit the unnecessary computation time in the concrete structures surrounding the reactor ZOE.

The last column of the following tables relative to a given dosimeter gives the percentage of the background noise compared to the direct signal, this last one being calculated by TRIPOLI-4. The second column gives the reaction

rates relative to the background noise and the third column the stochastic standard deviation resulting from the Monte Carlo method.

For the experiments on the bulk iron, the background noise considered in fast neutrons varies from 1/500 at short distance up to 1/200 at large distance. This estimated background noise reaches an order of 10 % for slow neutrons at very short distances and up to 1/200 at large distances.

X cm	Reaction rate (noise)	σ %	Noise/signal %
0.0	1.363E3	0.6	0.21
5.5	5.632E2	1.0	0.30
11.0	2.182E2	2.0	0.34
16.5	9.303E1	4.6	0.43
22.0	3.697E1	10	0.45
27.5	(1.249E1)	17	(0.44)

Background noise on P31 measurements

X cm	Reaction rate (noise)	σ %	Noise/signal %
0	1.306E5	0.26	0.22
10	6.448E4	0.74	0.29
20	3.459E4	0.85	0.33
30	1.935E4	1.2	0.36
40	1.109E4	2.4	0.38
50	6.624E3	2.7	0.41
60	4.009E3	3.7	0.43
70	2.707E3	5.3	0.49
80	1.566E3	7.6	0.48
90	9.141E2	4.3	0.46

Background noise on Si WIGNER measurements

X cm	Reaction rate (noise)	σ %	noise/signal %
0	6.497E4	0.28	0.22
10	2.520E4	0.65	0.29
20	1.077E4	1.3	0.33
30	4.847E3	1.9	0.35
40	2.367E3	2.3	0.37
60	7.493E2	4.9	0.44
80	2.494E2	7.0	0.47
100	8.613E1	7.2	0.47
120.	3.092E1	4.8	0.46

Background noise on Rh103 measurements

X cm	Reaction rate (noise)	σ %	noise/signal %
0	1.355E5	0.29	0.22
5	8.744E4	0.46	0.22
10	5.5832E4	0.68	0.29
15	3.557E4	0.93	0.31
20	2.369E4	1.3	0.34
25	1.590E4	2.0	0.36
35	6.896E3	2.0	0.36
45	3.702E3	3.0	0.41
55	1.984E3	5.3	0.44
70	9.070E2	7.2	0.51

Background noise on Np237 chamber measurements

X cm	Reaction rate (noise)	σ %	noise/signal %
0	1.439E5	0.85	10.4
2.24	1.452E5	1.0	7.0
5.0	1.257E5	1.6	4.48
6.72	1.100E5	1.1	3.44
10	9.028E4	1.2	2.44
16	6.206E4	2.3	1.54
20	4.788E4	2.0	
22	4.261E4	2.1	
26.5	3.318E4	2.0	0.87
30	2.593E4	2.8	0.71
32.16	2.653E4	2.5	0.77
37	2.015E4	2.4	0.65
42	1.732E4	3.0	0.62
46.5	1.491E4	3.1	0.61
52.1	1.273E4	3.6	0.59
56.5	1.044E4	3.6	0.56
62	8.625E3	2.7	0.53
67.5	7.186E3	3.2	0.52
73.4	6.301E3	3.8	0.54
78.28	5.690E3	4.1	0.58
83.52	4.706E3	4.5	0.54
88.76	3.877E3	5.2	0.54
94	3.121E3	4.0	0.51
99.24	2.660E3	4.9	0.54

Background noise on Mn/Cd measurements

X cm	Reaction rate (noise)	σ %	noise/signal %
104.48	2.186E3	4.4	0.52
110	1.768E3	4.4	0.49
119.96	1.199E3	5.1	0.49
130	8.459E2	5.6	0.54
135.44	5.868E2	5.7	0.52
140.68	4.101E2	7.5	0.52

Background noise on Mn/Cd measurements (continuation)

X cm	Reaction rate (noise)	σ %	noise/signal %
0	3.438E6	3.9	9.0
5	7.085E6	3.4	5.42
10	7.421E6	3.1	3.66
20	4.890E6	7.2	1.60
30	2.709E6	5.4	1.06
40	1.731E6	6.8	0.74
50	1.150E6	9.3	0.66
60	7.009E5	7.9	0.50
70	(7.026E5)	11	
80	(4.866E5)	11	

Background noise on In115/Cd measurements

X cm	Reaction rate (noise)	σ %	noise/signal %
0	5.022E6	3.3	12.8
5	8.570E6	2.7	5.91
10	7.455E6	2.8	3.23
16	5.711E6	3.9	2.10
30	2.479E6	5.2	0.92
40	(1.854E6)	11.	(0.81)
46.5	1.285E6	7.6	0.64
50	1.101E6	9.2	0.60
60	8.051E5	9.1	0.57
62	6.875E5	6.1	0.52
67.5	(6.946E5)	17.	(0.61)
70	5.678E5	7.6	0.54
77	4.842E5	8.1	0.57
91.92	3.024E5	9.2	0.54

Background noise on Au197/Cd measurements

X cm	Reaction rate (noise)	σ %	noise/signal %
0	2.515E6	0.51	1.95
5	2.577E6	0.59	2.11
10	2.051E6	0.85	1.70
15	1.485E6	0.78	1.28
25	8.470E5	1.1	0.86
50	2.960E5	1.7	056
70	1.539E5	1.7	0.53

Background noise on U235 chamber measurements

X cm	Reaction rate (noise)	σ %	noise/signal %
0	2.602E6	0.68	1.64
10	2.466E6	2.0	1.29
20	1.304E6	1.7	1.05
30	7.732E5	2.7	0.74
50	3.734E5	4.3	0.57
80	1.394E5	4.2	0.55
110	4.815E4	5.5	0.55

Background noise on Pu239 chamber measurements

V Conclusions

This TRIPOLI-4 interpretation of the "iron" benchmark of "NAÏADE 1" reveals three clear features:

1. By comparison with the experiment, the calculation underestimates the attenuation of the very fast neutrons (P31, table E-4) while the attenuations of the somewhat less energetic neutrons (WIGNER silicon, rhodium, Np237 fission chamber) appear to be well calculated (Tables E-5, E-6 and E-7).
2. The values of epithermal flux for short penetrations (Tables E-8, E-9 and E-10) are underestimated. This phenomenon may be due to a poor evaluation of the epithermal neutron background noise or use of an erroneous value for the boron concentration in the boral. The gold dosimeter, which is particularly reliable, gives very good results after 10 cm of penetration.
3. The responses of the U235 and Pu239 fission chambers do raise a problem: the calculation underestimates their response and does so uniformly in space over 2 decades of attenuation.

PART F

Experiments on the graphite mock-up

I Introduction: description of the experiment

Most of the measurements of fission neutron penetration into the graphite block were carried out early in 1965. The diameter of the boral diaphragm was 60 cm, although a few measurements were done using a 40-cm diaphragm. The dosimeters used involved the following reactions:

1. S32 (n,p)
2. Rh103 (n,n')
3. P31 (n,p) (2 sets of measurements)
4. 3 sets of measurements with silicon diodes (WIGNER effect)
5. Mn55 (n,γ) under cadmium
6. Mn55 (n, γ) (bare metal)
7. 2 sets of measurements using Au197 (n, γ) under cadmium, one at short distance, the other at longer distance with overlap
8. 2 sets of measurements using the In115 (n, γ) under cadmium.

Measurements were carried out to determine the absorption cross-section for thermal neutrons by the graphite used. A reproduction of page 19 of reference [1] sets out the experimental conditions and its translation is reproduced hereunder.

Experiments in graphite (translation relative to ref [1])

1) Characteristics

The specific gravity is d = 1.65
The thermal capture cross-section averaged over the Maxwell spectrum is: σ_a = 4.05 m barn

2) Description of the mock-up

The assembly is a block measuring 200 x 200 x 140 cm
It consists of 7 plates measuring 200 x 200 x 20 cm enclosed in a steel frame 1 cm in thickness. The frame gives stability and enables the block to be suspended from a beam.

3) Location of detectors

Each plate has a hole drilled at its centre (in line with the axis of the neutron source, diameter Ø= 5 cm). The hole can be stopped up with graphite plugs of the same diameter and thickness 5 cm or 2 cm. The detectors to be irradiated are positioned between these plugs.
Locations are known to within 1 mm by measuring the distance from the detector inserted to one of the surfaces of the plate.

4) Experiments carried out

These are shown in table 11.

5) Results

These are given in tables 11-1 to 11-4 and figure 9-1 to 9-5.

We are also able to supplement this information by the results of recent mass spectrometry measurements on the impurities present in graphite produced at the same time. This was the graphite used in the reflector of the gas-cooled natural uranium reactor of the CHINON A3 unit.

II Results and interpretation of the graphite experiments

Just as for the measurements done on other mock-ups placed in NAÏADE 1, we draw a distinction between two types of experimental results:

1. The so-called "as-measured" results: these are the conventional fluxes published in reference [1] in December 1970.
2. The so-called "corrected" results: these are the results we have re-evaluated in line with the principles set out in part B (§ 5). It is recalled that this re-evaluation is based on improvements in certain nuclear data made between 1965 and 2004; these nuclear constants have influenced earlier interpretations.

In the tables below, the as-measured results, the corrected results and those given by applying the TRIPOLI-4 Monte Carlo program are shown together for each type of dosimeter. The as-measured conventional fluxes are converted to the corrected fluxes by applying correction factors that are summarized in the following table where the factors for the activation dosimeters are taken from part B. As regards the equivalent WIGNER fission fluxes (silicon damage) the correction factor is calculated in part E which pertains to the iron mock-up.

Equivalent Mn and Mn/Cd (n, γ) thermal fluxes	**1.00**
Epithermal Au/Cd and In/Cd (n, γ) fluxes per unit of lethargy	**1.016**
Equivalent Rh102(n,n') fission fluxes	**0.815 ±0.04**
Equivalent S32(n,p) fission fluxes	**0.815 ±0.03**
Equivalent Np237 (n,f) fission fluxes	**0.815 or 1.00**
Equivalent P31 (n,p) fission fluxes	**0.815 ±0.01**
Equivalent WIGNER Si fission fluxes	**1.015 ±0.02**

The positions of the dosimeters placed between the graphite discs are known to within 0.1 cm [1]. No mention is made of the uncertainty about the specific gravity of the graphite. As regards its composition, we assumed the isotopic concentrations given by the spectrometer analysis and which involves significant thermal neutron capture. We then supplemented the composition with traces of B10 such that the total **Maxwellian** capture cross-section is 4.05 mb (per atom of graphite) as indicated in reference [1], page 19. Finally, the composition of the graphite used in the calculations done with the TRIPOLI-4 program is given in the following table in atoms per 10^{-24} cm^3. The Maxwellian capture cross-sections are taken from reference [8] with ENDF/B-VI for all the isotopes except lithium (clearly ENDF/B-VI includes an error) for which we use the value of JENDL-3.2.

C_GRAPHITE	**8.281E-2**
K	**2.268E-7**
N14	**2.83E-7**
L16	**1.24E-9**
CL	**1.822E-6**
B10	**8.78E-9**

The effective cross-sections used for interpreting the experiment by the TRIPOLI-4 program are all taken from the ENDF/B-VI R4 evaluation. For converting reaction rates into conventional fluxes we used the mean values of the cross sections over the fission spectrum σ_f, the resonance integrals I and the effective cross-sections at 2200 m/s σ_0 given below. These are coherent with the values of the effective point cross-sections used for calculating reaction rates in the interpretation by the TRIPOLI-4 program.

P31(n,p)	IRDF_90	σ_f=0.02858b	recalculated
Mn55(n,γ)	ENDF/B-VI/R4	σ_o=13.45	[8]
S32(n,p)	IRDF_90	σ_f=0.06524b	recalculated
Au197(n,γ)	IRDF_90	I=1565b	[8]
In115(n,γ)	EBDF/B-VI R4	I=3281b	[8]
Rh103(n,n')	IRDF_90	σ_f=0.7033b	recalculated
Np237(n,f)	ENDF/B-VI R4	σ_f=1.305b	[8]
WIGNER Si	[14]	σ_f=0.9970	[14] and recalculation

The cadmium cut-off was placed at 0.5 eV.

The geometry used in the TRIPOLI-4 calculations was determined as follows. The description of NAÏADE 1 used in part A was retained, with the experimental area containing the graphite mock-up. The latter was modelled by a graphite parallelepiped measuring 200 cm x 200 cm x 140 cm surrounded by a steel frame (containing 0.6% of carbon) and 1 cm in thickness. Along the axis Ox, we modelled a series of cylinders perpendicular to the axis, 5 cm in radius and of variable thickness. The adjoining surfaces of two consecutive cylinders are used to calculate the mean reaction rates on the discs of radius 5 cm. The mock-up therefore consists of the following volumes:

Air: volumes 428, 528, 628, 728 and 828
Mild steel: volumes 1528, 1628, 1728 and 1828
Graphite: volume 28 pierced by volumes 200 to 223

The TRIPOLI-4 calculation bears the reference 05_001; the source file is "naiadegraph_2005.data" in the directory /home/nimal/TRIPOLI-4/NAIADE_GRAPHITE/ in the nimal2 machine. The calculation covers 100 batches of 450,000 first generation fission neutrons with the FIXED_SOURCE_CRITICALITY option so that it is possible to use, as we have pointed out, the TRIPOLI-4 MONITORING option. The normalisation to first generation fission neutrons is still 1.70402E11n/s. The simulation lasted 808,750 seconds on a PC running at 2.7GHz.

The following table gives the number of neutrons emitted subsequent to and excluding the first generation (this is the fixed source subcritical mode whereby secondary neutrons can be born with their correct spatial and energy characteristics). The natural uranium converter was subdivided into two equal portions, each 1 cm in thickness:

1. Volume 11: ZOE reactor side (V11)
2. Volume 12: NAÏADE 1 void side (V12)

Volume	Isotope	Energy range	Number of neutrons/s	SD %
V11	**U235**	**20MeV-0.5eV**	**7.1238E8**	**0.074**
V11	**U235**	**0.5eV-0.**	**5.7218E8**	**0.24**
V11	**U235**	**20MeV-0.**	**1.2846E9**	**0.13**
V12	**U235**	**20MeV-0.5eV**	**7.7346E8**	**0.062**
V12	**U235**	**0.5eV-0.**	**5.1596E8**	**0.22**
V12	**U235**	**20MeV-0.**	**1.2894E9**	**0.10**
V11	**U238**	**20MeV-0.**	**1.08580**	**0.026**
V12	**U238**	**20MeV-0.**	**9.4688E9**	**0.026**
total		**20MeV-0.**	**2.2901E10**	

The generations beyond the first represent 13.44% additional neutrons.

The results are shown in the following tables where the columns headed "rate" correspond to microscopic reaction rates and the "flux" columns to conventional fluxes.

X cm	TRIPOLI-4 Rate	σ%	TRIPOLI-4 flux	As-measured results	Corrected data	C/E
0	1.484E6	0.73	2.275E7	2.60E7	2.12E7	1.07
5	7.309E5	1.23	1.120E7	1.30E7	1.06E7	1.06
10	3.990E5	2.00	6.116E6	6.81E6	5.55E6	1.10
15	2.219E5	2.59	3.401E6	3.87E6	3.15E6	1.08
20	1.308E5	2.98	2.005E6	2.22E6	1.81E6	1.11
25	7.565E4	3.23	1.160E6	1.24E6	1.01E6	1.15
30	4.351E4	3.90	6.669E5	7.57E5	6.17E5	1.08
35	2.631E4	3.88	4.033E5	4.30E5	3.50E5	1.15
40	1.524E4	3.65	2.336E5	3.00E5	2.45E5	0.96
45	(1.036E4)	11	(1.588E5)	1.69E5	1.38E5	1.15
50	(6.661E3)	13	(1.021E5)	7.60E4	6.19E4	1.65

Table F-1 (S32)

Table F-1 shows the response of the sulphur dosimeters. These were 2.5 mm in thickness. The experiment was carried out on 11/05/1965.

X cm	TRIPOLI-4 Rate	σ%	TRIPOLI-4 flux	As-measured results	Corrected data	C/E
0	2.831E7	0.37	4.025E7	4.56E7	3.72E7	1.08
5	1.502E7	0.63	2.136E7	2.43E7	1.98E7	1.08
10	8.503E6	0.94	1.209E7	1.35E7	1.10E7	1.10
15	4.842E6	1.31	6.885E6	7.62E6	6.21E6	1.11
20	2.781E6	1.55	3.954E6	4.25E6	3.46E6	1.14
25	1.561E6	1.29	2.220E6	2.56E6	2.09E6	1.06
30	9.112E5	1.91	1.296E6	1.40E6	1.14E6	1.14
35	5.308E5	1.94	7.547E5	8.93E5	7.28E5	1.04
40	3.061E5	2.19	4.352E5	4.64E5	3.78E5	1.15

Table F-2 (Rh103)

The above table F-2 gives the results of measurements made using the rhodium dosimeter carried out on 18/01/1965. The dosimeters were 0.2 mm in thickness.

X cm	TRIPOLI-4 Rate	σ%	TRIPOLI-4 flux	As-measured results 1	Corrected data 1	C/E
0	6.697E5	0.66	2.343E7	2.47E7	2.00E7	1.17
5	3.347E5	1.20	1.171E7	1.25E7	1.02E7	1.15
10	1.820E5	1.8	6.368E6	7.87E6	6.41E6	0.99
20	5.991E4	3.0	2.096E6	2.18E6	1.78E6	1.18
30	1.987E4	3.9	6.953E5	6.73E5	5.48E5	1.27
40	6.896E2	3.6	2.413E5	-	-	-

Table F-3 (P31 first set)

X cm	TRIPOLI-4 Rate	σ%	TRIPOLI-4 flux	As-measured results 2	Corrected data 2	C/E
0	6.697E5	0.66	2.343E7	2.58E7	2.10E7	1.11
5	3.347E5	1.20	1.171E7	-	-	-
10	1.820E5	1.8	6.368E6	7.13E6	5.81E6	1.10
20	5.991E4	3.0	2.096E6	2.18E6	1.78E6	1.18
30	1.987E4	3.9	6.952E5	7.46E5	6.08E5	1.14
40	6.896E2	3.6	2.413E5	2.67E5	2.18E5	1.11

Table F-4 (P31 second set)

The first set of measurements using the phosphorus dosimeter were carried out on 13/01/1965 and the second set on 12/05/1965, both using phosphorus dosimeters 3 mm in thickness.

Taken together, these four tables F-1 to F-4 show that the calculations of equivalent fission flux slightly overestimate the situation in absolute terms although no trend can be discerned as regards the linear attenuation coefficients of fast neutrons.

X cm	TRIPOLI-4 rate	σ %	AS MESURED results 1	2	3
0	**5.222E7**	**0.34**	**6.58E7**	**7.03E7**	**6.26E7**
5	**2.900E7**	**0.49**	**4.11E7**	**3.83E7**	**3.73E7**
10	**1.673E7**	**0.67**	**2.27E7**	**2.19E7**	**2.33E7**
15	**9.594E6**	**0.91**	**1.29E7**	**1.32E7**	**1.27E7**
20	**5.510E6**	**1.12**	**7.57E6**	**7.70E6**	**7.48E6**
25	**3.118E6**	**0.90**	**4.29E6**	**4.52E6**	**4.21E6**
30	**1.811E6**	**1.36**	**2.18E6**	**2.68E6**	**2.53E6**
35	**1.050E6**	**1.38**	**1.48E6**	**1.34E6**	**1.34E6**
40	**6.061E5**	**1.67**	**8.60E5**	**9.18E5**	**8.58E5**
45	**3.562E5**	**1.84**	**-**	**-**	**5.16E5**
50	**2.124E5**	**2.28**	**-**	**-**	**3.28E5**

Table F5 (as measured WIGNER Si)

These 3 measurements were carried out on 18 and 19 January 1965 (first and second sets)
and 11 and 12 January 1965 (third set). The three series of results are highly coherent. The appendix to part F sets out the coefficients used to convert from the spectrum to the equivalent WIGNER silicon "as-measured fission fluxes" (headed "rate" in table F5) as given in reference [14] as a function of neutron energy.

X cm	TRIPOLI-4 flux	σ %	CORRECTED results 1	2	3	C/E 1	2	3
0	**5.238E7**	**0.34**	**6.68E7**	**7.14E7**	**6.35E7**	**0.78**	**0.73**	**0.82**
5	**2.909E7**	**0.49**	**4.17E7**	**3.89E7**	**3.79E7**	**0.70**	**0.75**	**0.77**
10	**1.678E7**	**0.67**	**2.30E7**	**2.22E7**	**2.36E7**	**0.73**	**0.75**	**0.71**
15	**9.622E6**	**0.91**	**1.31E7**	**1.34E4**	**1.29E7**	**0.73**	**0.72**	**0.75**
20	**5.527E6**	**1.12**	**7.68E6**	**7.82E6**	**7.59E6**	**0.72**	**0.71**	**0.73**
25	**3.127E6**	**0.90**	**4.35E6**	**4.59E6**	**4.27E6**	**0.72**	**0.68**	**0.73**
30	**1.816E6**	**1.36**	**2.21E6**	**2.72E6**	**2.57E6**	**0.82**	**0.67**	**0.71**
35	**1.053E6**	**1.38**	**1.50E6**	**1.36E6**	**1.36E6**	**0.70**	**0.77**	**0.77**
40	**6.079E5**	**1.67**	**8.73E5**	**9.32E5**	**8.71E5**	**0.69**	**0.65**	**0.70**
45	**3.573E5**	**1.84**	**-**	**-**	**5.24E5**	**-**	**-**	**0.68**
50	**2.130E5**	**2.28**	**-**	**-**	**3.33E5**	**-**	**-**	**0.64**

Table F-5 bis (corrected WIGNER Si)

The relative attenuation of the equivalent WIGNER fission flux as a function of distance is well reflected by the calculation over 45 cm, but the values obtained by the calculation are systematically underestimated.

X cm	TRIPOLI-4 rate	σ %	TRIPOLI-4 flux	Mn/Cd Measurement	C/E
0	9.534E6	0.90	7.088E5	9.86E5	0.72
5	2.287E7	2.6	1.700E6	1.82E6	0.93
10	2.769E7	0.83	2.059E6	2.13E6	0.97
15	2.808E7	0.49	2.088E6	2.12E6	0.98
20	2.436E7	0.37	1.811E6	1.80E6	1.01
25	1.959E7	0.33	1.456E6	1.37E6	1.06
30	1.441E7	0.34	1.071E6	9.94E5	1.08
35	1.030E7	0.82	7.658E5	6.65E5	1.15
40	6.925E6	0.38	5.149E5	4.27E5	1.20
50	3.002E6	0.24	2.232E5	1.76E5	1.27
60	1.132E6	0.72	8.416E4	6.16E4	1.37
70	4.208E5	1.11	3.128E4	2.43E4	1.29
80	1.496E5	1.68	1.112E4	8.26E3	1.35
90	5.412E4	2.12	4.024E3	3.07E3	1.31
95	3.165E4	2.47	2.353E3	1.71E3	1.38
100	2.022E4	3.38	1.503E3	1.04E3	1.45
105	-	-	-	6.36E2	-
110	7.464E3	4.66	5.549E2	4.20E2	1.32
115	4.553E3	5.02	3.385E2	2.64E2	1.28
120	3.119E3	6.45	2.319E2	2.03E2	1.14

Table F-6 (Mn/Cd)

The measurements were carried out on 20/01/1965. As regards the response of the Mn/Cd dosimeter, which essentially integrates the epithermal neutrons, it can be seen that the calculation underestimates the equivalent thermal flux at short distances. At longer distances the calculation overestimates the results by about 30%.

X cm	TRIPOLI-4 rate	σ %	TRIPOLI-4 flux	Measurement 1	Measurement 2	C/E 1	C/E 2
0	3.975E7	0.34	2.955E6	3.58E6		0.83	
5	1.288E8	0.51	9.576E6	1.09E7		0.88	
10	1.969E8	0.23	1.464E7	1.65E7		0.89	
15	2.456E8	0.17	1.826E7	2.00E7		0.91	
20	2.754E8	0.20	2.048E7	2.20E7		0.93	
25	2.865E8	0.18	2.130E7	2.28E7		0.93	
30	2.852E8	0.22	2.120E7	2.33E7		0.91	
35	2.716E8	0.16	2.019E7	2.05E7		0.99	
40	2.524E8	0.17	1.877E7	1.90E7		0.99	
50	2.041E8	0.24	1.517E7	1.49E7		1.02	
60	1.563E8	0.17	1.162E7	1.14E7		1.02	
70	1.162E8	0.20	8.639E6	8.45E6		1.02	
80	8.472E7	0.22	6.299E6	5.30E6		1.19	
90	6.078E7	0.19	4.519E6	4.39E6		1.03	
100	4.316E7	0.28	3.209E6	3.09E6	3.03E6	1.04	1.06
105	-	-	-	2.53E6	2.53E6		
110	2.944E7	0.26	2.189E6	-	2.10E6		1.04
115	2.390E7	0.30	1.777E6	-	1.67E6		1.06
120	1.890E7	0.35	1.405E6	1.30E6	1.27E6	1.08	1.11
125	1.430E7	0.35	1.063E6	-	9.76E5		1.09
130	1.001E7	0.41	7.442E5	-	6.65E5		1.12
135	6.012E6	0.71	4.470E5	-	3.59E5		1.25
140	1.781E6	4.09	1.324E5	-	9.56E4		1.39

Table F-7 (bare Mn)

Measurements 1 and 2 were carried out on 19/01/1965 and 17/05/1965 respectively. The high reproducibility of the three measurements carried out four months apart (at distances 100, 105 and 120 cm) will be noted. The agreement between calculation and experiment is satisfactory apart from the calculated underestimate at very short distances and its underestimate of the leakage phenomenon at 140 cm.

X cm	TRIPOLI-4 rate	σ %	TRIPOLI-4 flux	As-measured results 1	Corrected data 1	C/E 1
0	6.401E8	2.06	4.090E5	5.20E5	5.28E5	0.77
5	1.917E9	1.35	1.225E6	1.26E6	1.28E6	0.94
10	2.704E9	1.17	1.728E6	1.69E6	1.72E6	1.01
15	2.973E9	1.07	1.900E6	1.99E6	2.02E6	0.94
20	2.818E9	1.13	1.801E6	1.92E6	1.95E6	0.92
25	2.436E9	1.23	1.557E6	1.70E6	1.73E6	0.90
30	1.983E9	1.48	1.267E6	1.14E6	1.16E6	1.09
35	1.419E9	1.23	9.067E5	8.30E5	8.43E5	1.08
40	1.010E9	1.62	6.454E5	6.04E5	6.14E5	1.05
50	4.589E8	2.23	2.932E5	2.46E5	2.50E5	1.17
60	1.768E8	2.42	1.130E5			
70	7.185E7	4.55	4.591E4			
80	2.162E7	5.32	1.381E4			
90	7.574E6	9.70	4.840E3			
100	2.825E6	14	1.805E3			

Table F-8 (Au 197/Cd(1))

X cm	TRIPOLI-4 rate	σ %	TRIPOLI-4 flux	As-mesured 2	Corrected data 2	C/E 2
0	6.401E8	2.06	4.090E5			
5	1.917E9	1.35	1.225E6			
10	2.704E9	1.17	1.728E6			
15	2.973E9	1.07	1.900E6			
20	2.818E9	1.13	1.801E6			
25	2.436E9	1.23	1.557E6			
30	1.983E9	1.48	1.267E6			
35	1.419E9	1.23	9.067E5			
40	1.010E9	1.62	6.454E5	6.50E5	6.60E5	0.98
50	4.589E8	2.23	2.932E5	2.07E5	2.10E5	1.39
60	1.768E8	2.42	1.130E5	1.10E5	1.12E5	1.01
70	7.185E7	4.55	4.591E4	3.02E4	3.07E4	1.50
80	2.162E7	5.32	1.381E4	1.28E4	1.30E4	1.06
90	7.574E6	9.70	4.840E3	4.85E3	4.93E3	0.98
100	2.825E6	14	1.805E3	2.10E3	2.13E3	0.85

Table F-9 (Au 197/Cd(2))

The gold dosimeters used on 1st and 2nd February 1965 consisted of gold deposits at 0.1 mg/cm^2. The C/E agreement is good except, again, at short distance where the calculated underestimate of the epithermal flux per unit of lethargy will be noted.

X cm	TRIPOLI-4 rate	σ %	TRIPOLI-4 flux	As-mesured 1	Corrected data 1	C/E 1
0	1.097E9	2.32	3.343E5			
5	3.416E9	1.39	1.041E6			
10	4.978E9	1.91	1.517E6			
15	5.774E9	1.56	1.760E6			
25	4.961E9	1.20	1.512E6			
30	4.060E9	1.11	1.237E6			
40	2.381E9	1.77	7.257E5			
50	1.070E9	1.33	3.261E5	2.43E5	2.47E5	1.32
60	4.307E8	1.94	1.313E5	9.90E4	1.01E5	1.31
70	1.713E8	3.07	5.221E4	3.82E4	3.88E4	1.35
80	5.942E7	4.46	1.811E4			
90	1.993E7	7.23	6.074E3	4.27E3	4.34E3	1.40
95	1.153E7	7.90	3.514E3	3.13E3	3.18E3	1.11
100	9.007E6	8.71	2.745E3	1.68E3	1.71E3	1.61
105	4.433E6	10.4	1.351E3	1.08E3	1.10E3	1.23

Table F-10 (In115/Cd (1))

X cm	TRIPOLI-4 taux	σ %	TRIPOLI-4 flux	As-mesured 1	Corrected data 1	C/E 2
0	1.097E9	2.32	3.343E5	4.76E5	4.84E5	0.69
5	3.416E9	1.39	1.041E6	1.03E6	1.05E6	0.99
10	4.978E9	1.91	1.517E6	1.53E6	1.55E6	0.98
15	5.774E9	1.56	1.760E6	1.63E6	1.66E6	1.06
25	4.961E9	1.20	1.512E6	1.32E6	1.34E6	1.73
30	4.060E9	1.11	1.237E6	1.10E6	1.12E6	1.11
40	2.381E9	1.77	7.257E5	5.63E5	5.72E5	1.27
50	1.070E9	1.33	3.261E5	2.55E5	2.59E5	1.26
60	4.307E8	1.94	1.313E5	9.50E4	9.65E4	1.36
70	1.713E8	3.07	5.221E4	3.96E4	4.02E4	1.30
80	5.942E7	4.46	1.811E4	1.48E4	1.50E4	1.20
90	1.993E7	7.23	6.074E3	6.22E3	6.32E3	0.96
95	1.153E7	7.90	3.514E3	2.80E3	2.84E3	1.24
100	9.007E6	8.71	2.745E3	1.69E3	1.72E3	1.60
105	4.433E6	10.4	1.351E3			

Table F-11 (In115/Cd (2))

The measurements were done on 25/01/1965 and 01/02/1965 respectively. As regards the response of the indium dosimeter encased in cadmium, which gives the flux per unit of lethargy at about 1.46eV, we may again note the calculated underestimate at the origin of the graphite block and an overestimate of greater distances.

III Background noise estimation using TRIPOLI-4 Code

A calculation of the background noise contribution due to the fast and epithermal neutrons (E > 0.5eV) stemming from the ZOE reactor core was made using the TRIPOLI-4 software. The Maxwellian thermal neutrons stemming from the ZOE's reflector cross the uranium converter then are absorbed by the thick borated screen. The determination of the neutron source generating the background noise is presented in the part D in front of the experiment descriptions.

Let us recall (see details in the table D-15) the levels of the experimental flux measurements in the following conditions:

1. Absence of the uranium converter carrying out the conversion of the thermal neutrons in fission neutrons.
2. Absence of the thick borated screen.
3. Diaphragm of 60cm.
4. Aluminium tank in place.
5. ZOE's power equal to 100kW.
6. Measurement in the axis of the converter on the internal face of the aluminium tank (x=y=z=0).

The experimental values of the neutron flux on the internal face of the tank are:

1. Thermal equivalent flux to 2200m / s 6.4E7
2. Flux by unity of lethargy 1.E4 to 2.E4
3. Equivalent fission flux 4.0E4 to 5.0E4

Let us also recall the order of the equivalent fission flux at the same point with, this time, the presence of the fission converter and the borated screen: 1.8E7

The results below are obtained with a source of background noise corresponding to that described in the paragraph IV-2 of part D. The neutrons are emitted only in a cone of axis Ox and from vertex angle Arccos (0.95) to limit the unnecessary computation time in the concrete structures surrounding the reactor ZOE.

The last column of the following tables relative to a given dosimeter gives the percentage of the background noise compared to the direct signal, this last one being calculated by TRIPOLI-4. The second column gives the reaction rates relative to the background noise and the third column the stochastic standard deviation resulting from the Monte Carlo method.

For the experiments on the bulk graphite, the background noise considered in fast neutrons varies from 1/500 at short distances up to 1/100 at large distances. This estimated background noise reaches several % for slow neutrons at very short distances and diminishes down to 1 % at large distances.

X cm	Reaction rate (noise)	σ %	noise/signal %
0	**1.457E3**	**0.72**	**0.22**
5	**9.028E2**	**1.35**	**0.27**
10	**5.733E2**	**2.83**	**0.32**
20	**2.517E2**	**8.5**	**0.42**
30	**(1.035E2)**	**23**	**(0.52)**

Background noise on P31 measurements

X cm	Reaction rate (noise)	σ %	noise/signal %
0	**1.111E5**	**0.60**	**0.21**
5	**7.330E4**	**0.79**	**0.25**
10	**4.626E4**	**1.19**	**0.28**
15	**3.345E4**	**1.46**	**0.35**
20	**1.847E4**	**3.15**	**0.34**
25	**1.093E4**	**5.86**	**0.35**
30	**6.703E3**	**9.78**	**0.37**
35	**(5.7E3)**	**20**	**from 0.4 to**
40	**(2.6E3)**	**28**	**0.5**

Background noise on Si WIGNER measurements

X cm	Reaction rate (noise)	σ %	noise/signal %
0	4.342E5	0.92	1.09
5	1.106E6	0.84	0.86
10	1.615E6	0.84	0.82
15	1.946E6	0.86	0.79
20	2.115E6	0.90	0.77
25	1.183E6	0.87	0.76
30	2.118E6	0.75	0.74
35	2.020E6	0.75	0.74
40	1.899E6	1.11	0.75
50	1.508E6	0.82	0.74
60	1.196E6	0.95	0.77
70	8.913E5	1.00	0.77
80	6.563E5	1.13	0.77
90	4.976E5	1.20	0.82
100	3.572E5	1.16	0.83
110	2.477E5	1.085	0.84
115	2.010E5	1.25	0.84
120	1.601E5	1.58	0.85
125	1.195E5	1.55	0.84
130	8.602E4	1.70	0.86
135	4.998E4	2.07	0.83
140	1.708E4	2.11	0.96

Background noise on Mn55 measurements

X cm	Reaction rate (noise)	σ %	noise/signal %
0	1.767E5	1.32	1.85
5	2.144E5	2.1	0.94
10	1.903E5	1.52	0.69
15	1.510E5	1.7	0.54
20	1.156E5	2.4	0.47
25	8.557E4	2.5	0.44
30	6.256E4	3.4	0.43
35	4.033E4	4.4	0.39
40	2.602E4	8.9	0.38
50	(1.264E4)	12.1	(0.42)
from 30 to 120			from 0.3 to 0.6

Background noise on Mn55/Cd measurements

X cm	Reaction rate (noise)	σ %	noise/signal %
0	6.103E4	0.60	0.22
5	3.920E4	0.86	0.26
10	2.450E4	1.41	0.29
15	1.886E4	2.01	0.39
20	9.722E3	4.09	0.35
25	5.383E3	6.48	0.34
30	(3.639E3)	13	(0.40)
35	(3.360E3)	24	(0.63)

Background noise on Rh103 measurements

X cm	Reaction rate (noise)	σ %	noise/signal %
0	3.221E3	0.79	0.22
5	1.985E3	1.54	0.27
10	1.250E3	2.69	0.31
15	(1.045E3)	29	0.47
20	5.480E2	8.66	0.42
from 25 to 35			from 0.4 to 1

Background noise on S32 measurements

X cm	Reaction rate (noise)	σ %	noise/signal %
0	1.397E7	4.95	1.27
5	4.039E7	7.23	1.18
10	4.222E7	3.47	0.85
15	4.117E7	3.78	0.71
25	2.652E7	4.11	0.53
30	2.073E7	4.69	0.51
40	8.938E6	5.41	0.38
from 50 to 80			#0.50

Background noise on In/Cd measurements

X cm	Reaction rate (noise)	σ %	noise/signal %
0	1.008E7	4.47	1.57
5	2.118E7	4.18	1.10
10	2.326E7	3.52	0.86
15	2.202E7	3.89	0.74
20	1.553E7	5.81	0.55
25	1.284E7	4.82	0.53
from 30 to 90			#0.50

Background noise on Au197/Cd measurements

IV Conclusions

Apart from the equivalent WIGNER fission flux which is underestimated by the calculation, the other equivalent fission fluxes for different distances in the graphite will be seen to be coherent. As in many experiments, the epithermal and equivalent thermal fluxes are underestimated by the calculation at very short distances. The estimation of the background noise does not explain this underestimation.

Appendix 1

This appendix taken from reference [14] gives the values of the silicon diode response. This response is practically normalised to unity over the fission spectrum.

Group number	Energies keV	σ_W
1	39.81 44.67	0.031692
2	44.67 50.12	0.036103
3	56.23	0.044086
4	63.10	0.057697
5	70.79	0.071372
6	79.43	0.070629
7	89.13	0.064564
8	100	0.057524
9	112.2	0.049324
10	125.9	0.041103
11	141.2	0.034051
12	158.5	0.051039
13	177.8	0.270495
14	199.5	0.773855
15	223.9	0.896541
16	251.9	0.693616
17	281.8	0.592772
18	316.2	0.543078
19	354.8	0.524501
20	398.1	0.515468
21	446.7	0.516135
22	501.2	0.538286
23	562.3	0.690572
24	631	0.661446
25	707.9	0.590859
26	794.3	0.771757
27	891.3	1.072576
28	1000	1.056910
29	1122	0.998794
30	1259	0.803576
31	1412	0.881572
32	1585	1.121863
33	1778	1.260419
34	1995	0.970823
35	2239	1.225842
36	2512	1.278700
37	2818	1.296587
38	3162	1.256097
39	3548	1.176366
40	3981	1.147436
41	4467	1.208185
42	5012	1.262449
43	5623	1.226772
44	6310	1.154334
45	7079	1.058763
46	7943	0.992619

(continued)

Group number	Energies keV	σ_w
47	**8910**	**0.969468**
48	**10000**	**0.987788**
49	**11220**	**1.020001**
50	**12590**	**1.061092**
51	**14100**	**1.109969**
52	**15792**	**1.130450**

REFERENCES

[1] M.LOTT, P. PEPIN, L. BOURDET, G. CABARET, J. CAPSIE, M. DUBOR, M. HOT, C. GOULET. Etude expérimentale de l'atténuation des neutrons dans différents matériaux de protection à l'aide du dispositif NAÏADE 1 du réacteur ZOE; CEA note 1386 December 1970

[2] J. BOURGEOIS, P. LAFORE. Dispositif experimental pour l'étude des protections. CEA Report 825.

[3] J. BRISBOIS, M. LOTT, G. MANENT. Mesure des flux de neutrons thermiques intermediares et rapides au moyen de détecteurs par activation; CEA Report R 2491 1964

[4] Private communication from D. BERETZ

[5] J. BUSSAC, P. REUSS. Traité de neutronique; collection enseignement des sciences, 25 Hermann

[6] J.C. NIMAL internal report SERMAL/LEPP/RT/00-2810/A

[7] J.H. BAARD, W.L. ZIJP and N.J. NOLTHENIUS. Nuclear DATA Guide for Reactor Nuclear Metrology. Kluwer Academic Publishers.

[8] OECD/NEA. Table of simple integral neutron cross-section data from JEF-2.2, ENDF/B-VI, JENDL-3.2, BROND-2 and CENDL-2.

[9] J.P. BOOTH, A. MAZZOLO, Y. PENELIAU, O. PETIT, B. ROESSLINGER. Notice d'utilisaiton du code TRIPOLI-4 version 4-3. Code de transport de particules par la méthode de Monte Carlo. DM2S. Report SERMA/LEPP/RT/01-2901-C

[10] P. LAFORE, J.P. MILLOT, J. RASTOIN. Puissance de la plaque d'uranium de NAÏAIDE. CEA Report 792.

[11] C. FICHE, G. MANENT, P. PEPIN. Report 832 (1967).

[12] MANDRAKESOFT Mandrake Linux 9.2. Mandrake Linux from A to Z.

[13] J. RASTOIN. Génie Atomique. Cours fondamental Tome II (extract printed separately) Ecrans de protection des réacteurs. Edition 1968.

[14] P. DULIEU Utilisation pratique du détecteur de dommages au silicium: CEA note 514, January 1965

[15] D. & M. FREMY QUID 2005, published by Robert Laffont